

Machine Learning Based Prediction and Optimization of Exergy Efficiency of Petroleum Refinery Under Uncertainty



By

Numan Sardar

(Registration No: 00000330357)

Department of Chemical Engineering

School of Chemical and Materials Engineering

National University of Sciences & Technology (NUST)

Islamabad, Pakistan

(2024)

Machine Learning Based Prediction and Optimization of Exergy Efficiency of Petroleum Refinery Under Uncertainty



By

Numan Sardar

(Registration No: 00000330357)

A thesis submitted to the National University of Sciences and Technology, Islamabad,

in partial fulfillment of the requirements for the degree of

Master of Science in
Process Systems Engineering

Supervisor: Dr. Iftikhar Ahmad

School of Chemical and Materials Engineering

National University of Sciences & Technology (NUST)

Islamabad, Pakistan

(2024)




THESIS ACCEPTANCE CERTIFICATE

Certified that final copy of MS thesis written by Mr Numan Sardar (Registration No 00000330357), of School of Chemical & Materials Engineering (SCME) has been vetted by undersigned, found complete in all respects as per NUST Statues/Regulations, is free of plagiarism, errors, and mistakes and is accepted as partial fulfillment for award of MS degree. It is further certified that necessary amendments as pointed out by GEC members of the scholar have also been incorporated in the said thesis.


Signature: 

Name of Supervisor: Dr Iftikhar Ahmad

Date: 09/08/2024

Signature (HOD): 

Date: 12/8/24

Signature (Dean/Principal): 

Date: 12/8/24



National University of Sciences & Technology (NUST)
MASTER'S THESIS WORK
Formulation of Guidance and Examination Committee

Form TH-1

Name: Numan Sardar

Department: Chemical Engineering

Credit Hour Completed: 24

Course Work Completed

NUST Regn No: NUST2020-MSPSE00000330357

Specialization: Process Systems Engineering

CGPA: 3.13

S/No	Code	Title	Core/Elective	CH	Grade
1	PSE-801	Process System Theory	Core	03	B+
2	PSE-852	Process Modeling and Simulation	Core	03	C
3	PSE-802	Optimization and Decision Analysis	Core	03	B
4	PSE-823	Advanced Process Dynamics and Control	Core	03	B+
5	TEE-820	Process Intensification	Elective	03	A
6	CSE-801	Computational Fluid Dynamics	Elective	03	B
7	EME-902	Numerical methods for CHE	Elective	03	B
8	EME-809	Wastewater Treatment and Design	Elective	03	B

Date: 15/02/2022

Student's Signature

Thesis Committee

- Name: Dr. Iftikhar Ahmad (Supervisor)
Department: SCME
- Name: Dr. Nouman Ahmad
Department: SCME
- Name: Dr. Erum Parvaiz
Department: SCME

Signature: _____

Signature: _____

Signature: _____

Date: 11/3/22

Signature of Head of Department: _____

APPROVAL

Date: 01-07-2022

Dean/Principal

Distribution

1x copy to Exam Branch, HQ NUST

1x copy to PGP Date, HQ NUST

1x copy to Exam branch, respective institute



Form: TH-04

National University of Sciences & Technology (NUST)

MASTER'S THESIS WORK

We hereby recommend that the dissertation prepared under our supervision by

Regn No & Name: 00000330357 Numan Sardar

Title: Machine Learning Based Prediction and Optimization of Exergy Efficiency of Petroleum Refinery Under Uncertainty.

Presented on: 18 Jul 2024 at: 1500 hrs in SCME

Be accepted in partial fulfillment of the requirements for the award of Master of Science degree in Process System Engineering.

Guidance & Examination Committee Members

Name: Dr Nouman Ahmad

Signature: [Signature]

Name: Dr Erum Pervaiz

Signature: [Signature]

Supervisor's Name: Dr Iftikhar Ahmad

Signature: [Signature]

Dated: 29/07/2024

[Signature]
Head of Department
Date 2/8/24

[Signature]
Dean/Principal
Date 5/8/24

School of Chemical & Materials Engineering (SCME)

AUTHOR'S DECLARATION

I **Numan Sardar** hereby state that my MS thesis titled “**Machine Learning Based Prediction and Optimization of Exergy Efficiency of Petroleum Refinery Under Uncertainty**” is my own work and has not been submitted previously by me for taking any degree from National University of Sciences and Technology, Islamabad or anywhere else in the country/ world.

At any time, if my statement is found to be incorrect even after I graduate, the university has the right to withdraw my MS degree.

Name of Student: Numan Sardar

Date: August 13, 2024

PLAGIARISM UNDERTAKING

I solemnly declare that the research work presented in the thesis titled “**Machine Learning Based Prediction and Optimization of Exergy Efficiency of Petroleum Refinery Under Uncertainty**” is solely my research work with no significant contribution from any other person. Small contribution/ help wherever taken has been duly acknowledged and that complete thesis has been written by me.

I understand the zero-tolerance policy of the HEC and the National University of Sciences and Technology (NUST), Islamabad towards plagiarism. Therefore, I as an author of the above-titled thesis declare that no portion of my thesis has been plagiarized and any material used as reference is properly referred/cited.

I undertake that if I am found guilty of any formal plagiarism in the above-titled thesis even after the award of MS degree, the University reserves the right to withdraw/revoke my MS degree and that HEC and NUST, Islamabad have the right to publish my name on the HEC/University website on which names of students are placed who submitted plagiarized thesis.

Student Signature:  _____

Name: Numan Sardar

DEDICATION

I dedicate this thesis to my parents, who have provided unwavering support, motivation, and love throughout my academic journey.

ACKNOWLEDGEMENTS

I extend my most profound appreciation to the Almighty Allah for providing me with the strength, guidance, and knowledge to complete this thesis. Furthermore, I'm eternally grateful for the boundless resources and wisdom bestowed upon me.

I want to express my sincere gratitude to my research supervisor, Dr. Iftikhar Ahmad, for his unwavering support, guidance, and compassionate counselling throughout my research journey. I am also grateful to my thesis committee members, Dr. Nouman Ahmad and Dr. Erum Pervaiz, for their insightful recommendations and valuable contributions.

I would also like to thank **Prof. Dr. Amir Azam Khan** (Principal School of Chemical and Materials Engineering) and **Dr. Erum Pervaiz** (HOD Department of Chemical Engineering) for providing a research oriented platform to effectively utilize my skills in accomplishing this research work.

Last, I want to express my most profound appreciation to my parents, family, and friends for their constant support and encouragement throughout my academic journey. Without their love and support, this accomplishment would not have been possible.

Numan Sardar

TABLE OF CONTENTS

ACKNOWLEDGEMENTS	ix
TABLE OF CONTENTS	x
LIST OF TABLES	xii
LIST OF FIGURES	xiii
NOMENCLATURE	xiv
ABSTRACT.....	xvi
CHAPTER 01: INTRODUCTION	1
1.1 Background.....	1
1.2 Exergy analysis in process industries	3
1.3 Thesis outlines	4
CHAPTER 02: LITERATURE REVIEW.....	5
2.1 Literature review.....	5
2.2 Significance of exergy analysis in petroleum refining	8
2.3 Uncertainty analysis techniques in refinery optimization.....	8
2.4 Research gap	9
2.5 Objectives	10
CHAPTER 03: PROCESS DESCRIPTION AND METHODOLOGY	11
3.1 Process description.....	11
3.2 Exergy analysis formulation	21
3.2.1 Exergy performance indicator.....	22
3.3 Artificial neural network (ANN)	23
3.3.1 The LM method	26
3.3.2 The scaled conjugate method.....	26
3.4 Genetic algorithm (GA)	27
3.4.1 Genetic operations	28

3.5	Particelle swarm optimization (PSO).....	31
3.6	Methodology	32
CHAPTER 04: RESULTS AND DISCUSSION.....		37
4.1	Steady state exergy analysis of petroleum refinery	37
4.1.1	Stream wise exergy analysis	37
4.1.2	Exergetic improvement potential and irriversibility	42
4.1.3	Exergy efficiency	43
4.2	Data based modelling and optimization.....	44
4.2.1	ANN training validation and perdition of exergy efficiency	44
4.2.2	GA and PSO based optimization.....	46
4.2.3	Optimization of exergy efficiency	49
CHAPTER 05: CONCLUSIONS.....		53
REFERENCES		54

LIST OF TABLES

Table 3.1: Time span of operations occurring in Delayed Coking Unit.....	20
Table 3.2: Chromosomes.....	28
Table 4.1: Input streams physical exergies.....	37
Table 4.2: Output streams physical exergies.....	39
Table 4.3: Genetic algorithm parameters used to optimize the exergy efficiency	47
Table 4.4: PSO parameters used to optimize the exergy efficiency	49
Table 4.5: Comparison of exergy efficiency of the process for GA and PSO.....	50

LIST OF FIGURES

Figure 1.1: American petroleum refinery's potential for energy savings [1]	2
Figure 3.1: Block flow diagram of a Petroleum refinery	12
Figure 3.2: Structure of neuron	24
Figure 3.3: Structure of Artificial Neural Network (ANN)	24
Figure 3.4: Schematic representation of Genetic Algorithm [29]	27
Figure 3.5: Roulette wheel selection.....	29
Figure 3.6: Selection of the Tournament.....	29
Figure 3.7: Single point cross over	30
Figure 3.8: Double point crossover.....	30
Figure 3.9: Uniform crossover.....	30
Figure 3.10: Flowchart of particle swarm optimization.....	32
Figure 3.11: Methodology	33
Figure 3.12: Data generation under uncertainty	34
Figure 4.1: Input streams with low physical exergies.....	38
Figure 4.2: Input Streams with high physical exergies.....	39
Figure 4.3: Output streams with low physical exergies	41
Figure 4.4: Output streams with high physical exergies	42
Figure 4.5: Exergetic improvement potential compared to irreversibility	43
Figure 4.6: Steady state exergy efficiency of the system	44
Figure 4.7: Predicted Vs actual exergy efficiency of training, testing and validation	45
Figure 4.8: Validation performance	46
Figure 4.9: Comparison of exergy efficiency for steady state, GA, Aspen validated model	51
Figure 4.10: Comparison of exergy efficiency for steady state, PSO, Aspen validated model	52

NOMENCLATURE

φ	Activation function
η	Exergy efficiency
AI	Artificial intelligence
ANN	Artificial neural networks
B_k	Bias
EX_{che}	Chemical exergy
EX_{ph}	Physical exergy
EX_{sys}	Total exergy of the system
$EX_{destroyed}$	Exergy destruction
EX_{feed}	Feed exergy
EX_{heat}	Heat exergy
EX_{in}	Exergy in
EX_{out}	Exergy out
EX_{ph}	Physical exergy
$EX_{product}$	Product exergy
EX_s	Total exergy of stream
f	Activation function
GA	Genetic algorithm
h	Enthalpy
h_0	Standard enthalpy
I	Irreversibility
IP	Improvement potential

\dot{m}	Mass flow rate
RMSE	Root means squared error
P	Pressure
P_0	Standard pressure
Q_c	Heat duty of condensor
Q_r	Heat duty of reboiler
R^2	Coefficient of determination
S	Entropy
S_0	Standard entropy
T	Temperature
T_0	Standard temperature
T_c	Temperature of condensor
T_r	Temperature of reboiler
w_i	Weights
x_i	Inputs
X_i	Mole fraction
Y_i	Predicted value

ABSTRACT

Energy efficiency studies are significant in the petroleum refinery because of their environmental impact and cost. In this context, crude distillation along with downstream units play an important role in refinery operations. This study established integrated frameworks that combine artificial neural networks (ANN) with particle swarm optimization (PSO) and genetic algorithm (GA). The objective was to achieve improved exergy efficiency in petroleum refinery operations under uncertainty. At first, a steady state Aspen HYSYS model was taken to execute the exergy analysis in order to measure the exergy efficiency, exergy destruction or irreversibility, and exergetic improvement potential of the overall plant model. The plant model was subsequently converted into a dynamic mode by initiating a $\pm 10\%$ uncertainty in the process parameters, such as pressure, temperature, and mass flow rates of 12 input streams. This resulted in the creation of a dataset consisting of 500 samples. Those datasets were utilized to create an Artificial Neural Network (ANN) model for the purpose of predicting the exergy efficiency. The ANN model was employed as a surrogate in Particle Swarm Optimization (PSO) and Genetic Algorithm (GA) environments to get superior exergy efficiency in the presence of uncertainty. The optimum process condition obtained using GA and PSO approach were fed into the Aspen HYSYS model for validation. The steady state exergy efficiency of overall petroleum refinery model was 72.38%, while the irreversibility or exergy destruction and improvement potential of the overall plant wide model was 7311.97 kW and 2037.85 kW respectively. The ANN was trained using the scaled conjugate backpropagation (**trainsecg**) training algorithm, with the network's activity being regulated by the **tansig** activation function. The RMSE was used to quantify the performance of the model architecture, having RMSE of 1.1349 for exergy efficiency. The R value for training is 0.99925, for validation is 0.93288, and for testing 0.91209. The performance of the particle swarm optimization (PSO) and genetic algorithm (GA) techniques were comparable, and they greatly improved the exergy efficiency of the overall plant compared to the steady state Aspen HYSYS model of the process.

Keywords: Exergy efficiency, Artificial neural network (ANN), Exergetic improvement potential, Exergy destruction, Machine learning, Particle swarm optimization (PSO), Genetic algorithm (GA).

CHAPTER 01: INTRODUCTION

1.1 Background

As the petroleum refinery sector utilizes an extensive amount of energy, a highly energy-efficient design needs to be implemented to make the industry viable and sustainable. Research started to focus on operations that are more energy efficient. Diesel, kerosene, naphtha, catalytic crackers, hydrocrackers, reformers, isomerization, and alkylation units are the principal refinery processing units. Petroleum refineries are known for their high energy intensity, which is mostly due to the complex and energy-intensive processes required in converting crude oil into viable refined products. A number of factors contribute to this energy level. To get started, the primary process of crude oil distillation takes a substantial amount of energy to heat the crude oil to high temperatures and keep it there throughout the distillation columns. Furthermore, hydro-processing components, such as hydrocrackers and hydrotreaters, are required to remove impurities and transform heavier hydrocarbons into lighter, more valuable compounds. These types of equipment work at high pressures and temperatures, requiring a significant amount of energy.

The US Department of Energy states that if existing RD-based technologies are implemented effectively in US oil refineries, 794 TBTU/year (26%) of energy may be recovered [1]. Potential energy-saving measures in the petroleum refinery are shown in Figure 1.1. The primary energy-saving options in reactive units, such as catalytic reforming, coking, isomerization, hydrocracking, and hydrotreating, are shown in Figure 1.1. Therefore, increasing the processes' energy efficiency is always desired to increase their viability and sustainability.

There are two general categories into which the examination of energy loss identification and possible improvement can be separated. One is grounded in traditional energy analysis, which assesses the quantity of energy lost in relation to the quantity of energy input without taking into account the energy's quality or ability to propel a process. It does this by relying only on the first law of thermodynamics.[1]. The other, however, is based on exergy analysis, which combines the principles of thermodynamics 1 and 2 to determine the process's actual thermodynamic improvement potential [2], [3].

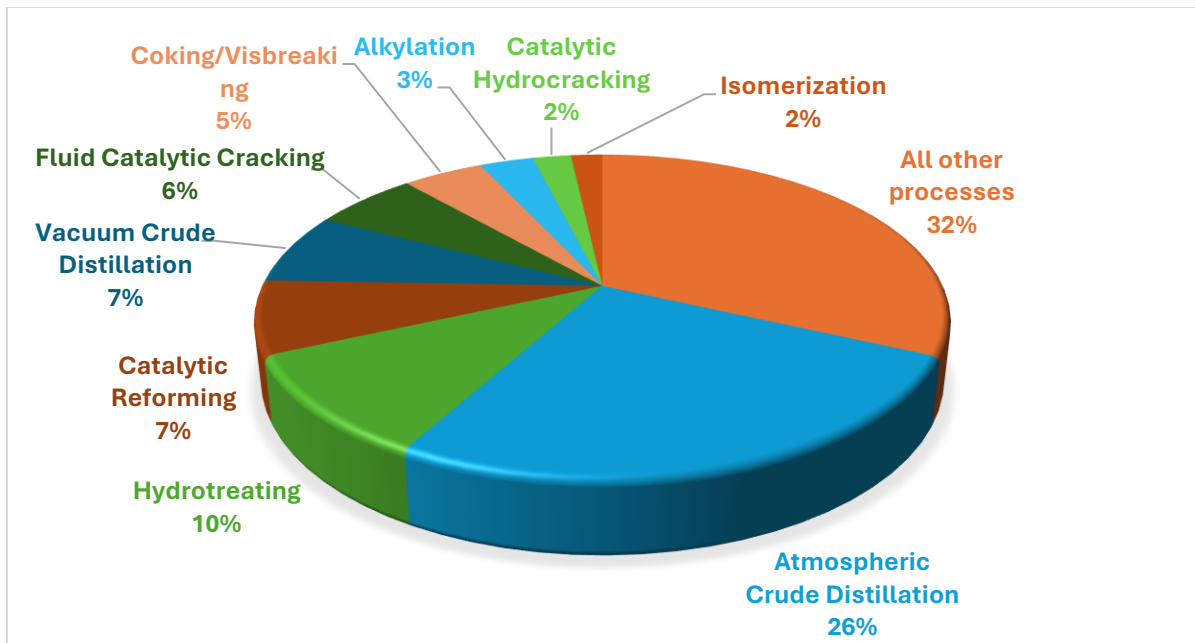


Figure 1.1: American petroleum refinery's potential for energy savings [1]

Energy analysis provides definite advantages over standard energy analysis for evaluating the energy efficiency of petroleum refineries. Energy analysis takes into account the quality of energy in contrast to traditional energy analysis, which only looks at energy quantity. It assesses the ability of various energy sources to carry out beneficial tasks while taking variations in chemical composition, pressure, and temperature into consideration. This distinction is particularly important in refineries since different processes require different grades of energy, and energy quality can vary greatly there.

Energy analysis is a highly effective tool for identifying inefficiencies in refinery operations. Engineers and operators can more effectively target areas for improvement by pinpointing the precise sites where energy losses occur, as opposed to energy analysis, which may merely disclose total energy inefficiencies without identifying their source. With this accuracy, refineries can make well-informed decisions regarding equipment upgrades, process modifications, and operational adjustments that will lower energy losses and improve overall efficiency.

Additionally, energy analysis supports initiatives aimed at environmental sustainability. Refineries must not only limit their environmental impact but also cut down on energy use in the modern, eco-aware world. Refineries can concurrently reduce greenhouse gas emissions and other environmental effects related to energy generation and consumption by lowering exergy losses.

1.2 Exergy analysis in process industries

In the relentless pursuit of efficiency, process industries constantly seek ways to optimize their energy consumption. Here's where exergy analysis steps in, offering a more nuanced perspective compared to traditional energy analysis. While traditional methods track the total energy flowing through a process, exergy analysis focuses on the quality, or usability, of that energy. Imagine energy as a spectrum, with high-grade, usable potential for work at one end and unusable waste heat at the other. Exergy analysis helps quantify how much of the incoming energy stream resides in this high-grade, usable zone (exergy) and how much inevitably degrades towards the unusable end (exergy destruction) as the process progresses towards equilibrium with its surroundings.

Exergy analysis is widely studied in order to evaluate, design, and maximize the efficiency of a variety of industrial processes, including petrochemical [4], chemical [5], sugar [6], cement [7], steel [8], and pulp and paper [9]. However, because modeling tasks are difficult and computationally intensive, the exergy calculation approach struggles to handle uncertainty in process circumstances. The goal of this research is to create a computational model that can effectively be used to manage uncertainty in the chemical industries' developing or operating stages. This tool is flexible enough to be adjusted as needed, yet rigorous enough to handle the intricate computations needed for energy analysis. This focus on quality becomes particularly valuable when pinpointing inefficiencies. Traditional analysis might reveal high overall energy consumption, but exergy analysis acts like a spotlight, illuminating the specific process steps where valuable exergy is being squandered. For instance, consider a distillation process where high-temperature steam condenses to heat a product stream. Traditional analysis might show the total energy used to generate the steam. Exergy analysis, however, would delve deeper, revealing the initial exergy content of the steam (a function of its temperature and pressure) and how much of that potential for work is lost during condensation. This loss occurs because the temperature difference between the steam and the product stream limits the amount of usable work that can be extracted. By quantifying this exergy destruction, engineers gain valuable insights. They can identify bottlenecks in the process, like poorly insulated equipment that allows excessive heat loss, or inefficiencies in heat exchanger design that prevent full utilization of the steam's exergy content.

The benefits of exergy analysis extend beyond pinpointing inefficiencies. When evaluating different process designs or modifications, it allows for a more accurate comparison of their

true efficiency. By considering not just the total energy consumption but also the quality of the energy used, exergy analysis helps engineers choose the option that offers the most efficient use of resources. This can lead to significant cost savings, particularly in industries where energy costs are a major factor. Additionally, exergy analysis paves the way for a more sustainable future. By revealing exergy destruction points, it empowers process engineers to explore opportunities for process redesign, the integration of heat recovery systems, or even the utilization of renewable energy sources with a higher exergy content. This holistic approach to energy management minimizes exergy destruction, leading to a more sustainable and cost-effective operation for process industries.[4]

1.3 Thesis outlines

The following is the arrangement of the thesis. Background information is given in the first chapter, followed by the literature review in 2nd chapter. The research method employed to build the framework for forecasting and maximizing exergy efficiency is covered in Chapter 3. The results and discussions about the optimization methods and exergy quantification are presented in Chapter 4.

CHAPTER 02: LITERATURE REVIEW

2.1 Literature review

Petroleum refineries convert crude oil, an unprocessed substance derived from the Earth, into a diverse array of valuable commodities. The refining process involves a sequence of intricate procedures, such as distillation, cracking, reforming, and treating, to manufacture a range of petroleum products, including petrol, diesel fuel, jet fuel, petrochemicals, and others. Refineries play a crucial role in addressing the global energy and industrial demands by providing critical goods that power transportation, industry, and manufacturing.

The intricate operations are highly energy-intensive, accounting for 33% of the overall energy consumption in the industrial sector. Enhancing the energy efficiency of processes is consistently sought after to enhance their viability and sustainability. The analysis to identify energy losses and potential areas for improvement can be categorized into two main techniques. The first approach is based on conventional energy analysis, which utilises the principles of the first law of thermodynamics. On the other hand, the second method utilises exergy analysis, which combines the principles of the first and second laws of thermodynamics to uncover the actual thermodynamic enhancement possibilities within the process.

Numerous exergy analysis-based research on different petroleum refinery processes have been published. For example, when Portha et al. [10] used life cycle assessment in conjunction with exergy analysis to study naphtha reforming, they discovered that heat exchangers were the primary cause of exergy destruction. Mustafa et al. [11] carried out additional research in the reactors of naphtha reforming unit. For the reason of the high chemical potential of the products, the exergy study along the length of the reactor revealed that as reactor length rose, chemical exergy increased while physical and mixing exergy declined.

Energy and exergy study of the fluid catalytic cracking unit (FCCU) of the Kaduna refining and petrochemical company (KRPC) was done by Nuhu et al. (2012) [12]. Aspen V.7 was used to create the model utilising industrial data. The unit's overall energy efficiency was a mere 24.7%. They discovered that 67% of the total exergy was destroyed by the fractional columns, which were the main source of exergy destruction. Petar et al. (2014) [13] conducted an exergy analysis on the separation section of FCCU through the use of computational modelling. With an energy destruction rate of 105 GJ/h, they discovered a fractionation column with a great

potential for energy optimisation. They also lower the total irreversibility by 10% in the separation stage by making several topological modifications. Al-Mutairi performed energy and retrofit study on FCCU using the heat recovery technology as a decision benchmark. In contrast to the current 109 °C, he suggested that the ideal ΔT_{\min} be 20 °C, which would reduce process energy losses from 9.11 MW to 3.83 MW. Agbo et al. (2019) replicate the Naptha hydrotreating unit of KRPC using industry data. After that, exergy analysis was used to determine that the main causes of exergy losses were strippers, heat exchangers, and heaters (17.4%, 14.6%, and 21.6%, respectively). It was discovered that 36.2% of the energy was destroyed in NHU overall.

A three-link structural model is introduced by Chen et al. [14] to lower the energy and exergy losses of Chinese refineries. Based on the energy use characteristics of the structural model, the model predicted energy-saving actions that resulted in a 37.2% reduction in energy consumption in the delayed coking unit. A unique approach to exergy analysis was presented by Lei et al. [15] in an integrated fractionating and heat exchanger delayed coker process. With the idea of preventable and unavoidable energy destruction, it is based on an enhanced energy level composite curve that offers a more precise analysis of process energy use. According to their findings, the component with the lowest energy efficiency was 29.4%. The greatest possibility for improvement is seen in the heat exchange between petrol oil and de-ethanization petrol.

Chegine et al. conducted a steady state analysis of the energy expenditure in hydrocracking and discovered that the reaction section's large pressure drop and the flue gas exhaust are the process's main sources of energy loss. Using an exergy analysis on an amine regeneration unit, Ibrahim et al. found that the regenerators were responsible for 80% of the process's exergy destruction. Exergy and pinch analysis were performed by Bandyopadhyay et al. on diesel hydrotreating units with two distinct layouts: the hot separator layout and the cold separator layout. They discovered that letdown valves, air coolers, and fired heaters can all be used to increase exergy efficiency.

The use of a data-based technique for energy analysis on different process units has also been documented in the present trend of artificial intelligence (AI) applications in process industries. An exergy efficiency prediction machine-learning model was created by Arif et al. Initially, they conducted a steady state exergy analysis and discovered that the furnace operating at a

high temperature was the most exergetic. Next, using data created on artificial uncertainty in the Elven process condition of the first primary model, they produced an ANN model.

In a different work, M. Khan et al. [16] created a straight run (SR), Genetic Algorithm (GA) and Artificial Neural Network (ANN) models to investigate the impact of uncertainty in the composition of the crude and some process parameters on the furnace's losses and exergy efficiency while maintaining a constant mass flow rate of fuel, oil, and excess air. In order to forecast vacuum distillation unit (VDU) exergy efficiency under elven uncertain process conditions, Kurban et al. [17] created machine learning models.

Initially, a sensitivity analysis was conducted to examine the impact of various process parameters on exergy efficiency. The temperature of the exit furnace was found to have the greatest influence. They then created and contrasted random forest (RF) and bootstrap aggregating (bagging) models to examine how process conditions affect exergy efficiency. A statistical model based on bootstrap filter (BF) and random forests (RF) was created by Akram et al. [18] to investigate the impact of uncertain process parameters on the overall plant exergy efficiency of naphtha reforming. Additionally, they used ANN and genetic algorithms to create an optimization method. An intelligent method is developed by Samad et al. [19] to forecast the exergy efficiency of the integrated naphtha reforming and isomerization processes. To determine the process's exergy efficiency, irreversibility, and room for improvement, they first carried out a steady state exergy analysis. then used MATLAB and Aspen Hysys integration to create data samples with artificial uncertainty, which were then used to train and test the ANN model. In another research project, Samad et al. [20] optimized the process' energy efficiency under uncertainty by using the intelligent model as a surrogate in the PSO and GA environments. By running the Aspen HYSYS model on the ideal situation produced by PSO and GA and determining the absolute error, they were able to validate their findings. The results show that the framework was dependable and effective.

Although numerous research studies have been published on the steady state exergy analysis of various processes of petroleum refinery, but no work has been reported on the exergy analysis of petroleum refinery under uncertainty to the best of the author's knowledge. Furthermore, no work has been done to optimize the exergy efficiency of petroleum refinery under uncertainty.

2.2 Significance of exergy analysis in petroleum refining

Exergy analysis holds immense significance in the realm of petroleum refining due to its ability to provide detailed insights into the energy utilization, efficiency, and sustainability of refining processes. Within petroleum refineries, where energy consumption is substantial and environmental considerations are paramount, exergy analysis serves as a fundamental tool for optimizing operations and reducing resource wastage.

Firstly, exergy analysis allows engineers to dissect the energy flows within various refining units, such as distillation towers, catalytic crackers, and hydrotreaters, by quantifying the available work potential of energy inputs and outputs. This comprehensive assessment helps identify areas of exergy destruction or inefficiencies within the system, shedding light on where energy losses occur and where improvements can be made. By understanding the sources of exergy destruction, refineries can implement targeted strategies to enhance energy efficiency, such as optimizing operating conditions, improving heat integration, or implementing advanced process technologies.[21], [22]

Moreover, exergy analysis aids in the evaluation and comparison of different process configurations and technologies, enabling refineries to make informed decisions regarding investment choices and resource allocation. For instance, by quantifying the exergetic performance of alternative refining processes or equipment, engineers can identify the most efficient and environmentally sustainable options. Additionally, exergy analysis can guide the integration of innovative solutions, such as waste heat recovery systems, cogeneration, or renewable energy sources, to further improve overall efficiency and reduce environmental impacts. Furthermore, exergy analysis supports the broader goals of sustainability and environmental stewardship within the petroleum industry. By minimizing energy consumption and optimizing resource utilization, refineries can reduce greenhouse gas emissions, mitigate environmental pollution, and enhance their overall environmental performance. This aligns with regulatory requirements, corporate sustainability initiatives, and societal expectations for responsible resource management and energy conservation.[23], [24]

2.3 Uncertainty analysis techniques in refinery optimization

Uncertainty analysis is a crucial aspect of refinery optimization, as refineries operate in an environment with numerous uncertainties, such as crude oil quality, product demand, and

market prices. Several techniques have been employed to address these uncertainties in refinery production planning.

One approach is the use of stochastic programming, which models uncertain parameters as random variables with known probability distributions. This allows for the optimization of expected performance while considering the risk associated with uncertain inputs.[25] Chance-constrained programming is another technique that ensures constraints are satisfied with a specified probability, accounting for the inherent uncertainties.[25]

Robust optimization is another method that seeks to find solutions that are optimal under the worst-case realization of the uncertain parameters. This approach aims to generate solutions that are less sensitive to variations in the input parameters.[25] Additionally, integration of the hydrogen network and utility system with the material balance optimization can improve the overall refinery optimization under uncertainty.[26]

These advanced uncertainty analysis techniques, combined with integrated refinery models, enable refineries to make more informed decisions, optimize production, and improve profitability while accounting for the various uncertainties they face.[25], [26], [27]

2.4 Research gap

The research gap that was observed from literature review are given in the following keypoints below,

- In 1950s the foundation of Exergy Analysis was laid by Keenan and Rant as a base of process analysis.
- The Exergy Analysis is done by the Matlab code, MS Excel or by integration of visual basic code with MS-Excel.
- The Exergy analysis of Petroleum refinery has been done only on specific unit processes till now.
- For petroleum refinery, steady state exergy analysis has been carried out but no work is reported under uncertainty, and optimization.

2.5 Objectives

The objectives of the thesis are given below,

- Development of an artificial intelligence-based model to study the effect of uncertainty on exergy efficiency.
- Optimization of the process using the integration of genetic algorithm and artificial neural network.
- To employ an ANN model as a surrogate in PSO and GA frameworks for achieving higher exergy efficiency of the overall plant under uncertainty.

CHAPTER 03: PROCESS DESCRIPTION AND METHODOLOGY

3.1 Process description

Petroleum refineries are intricate industrial structures consisting of various essential processes, each fulfilling a unique function in the conversion of crude oil into valuable petroleum products. The Crude Distillation Unit (CDU) is the central section of the refinery, responsible for separating crude oil into various fractions based on their boiling points. Subsequently, these fractions, which encompass gasoline, diesel, and other substantial goods, undergo additional processing in diverse conversion units. The Catalytic Cracking Unit (FCCU) uses a catalyst to decompose large hydrocarbon molecules into smaller products, whereas the Hydrocracking Unit uses hydrogen to transform heavy raw materials into more value gasoline and diesel fuel. In addition, Coking Units utilize thermal cracking to convert heavy residual oils into lighter products such as gasoline, diesel, and petroleum coke. Treatment units, such as the Hydrotreating Unit, are essential for eliminating sulfur, nitrogen, and other contaminants from refined products. This process ensures that the products meet environmental laws and enhances their quality. Supporting refinery operations are auxiliary facilities, which encompass utilities for steam generation and cooling water provision, along with tankage for storing both crude oil and finished products. Product blending facilities amalgamate different refined goods to fulfill market requirements, while distribution systems convey products to end-users through pipelines, tankers, trucks, and railcars. Control and safety systems, which include process control systems and safety measures, are crucial for preserving operational efficiency and guaranteeing a secure working environment within the refinery. These components combine to create a complete framework that allows petroleum refineries to effectively refine crude oil and manufacture a wide variety of important petroleum products. Figure 3.1 illustrates the schematic representation of a petroleum refinery. The flowsheet is derived from the Aspen HYSYS model of a petroleum refinery.

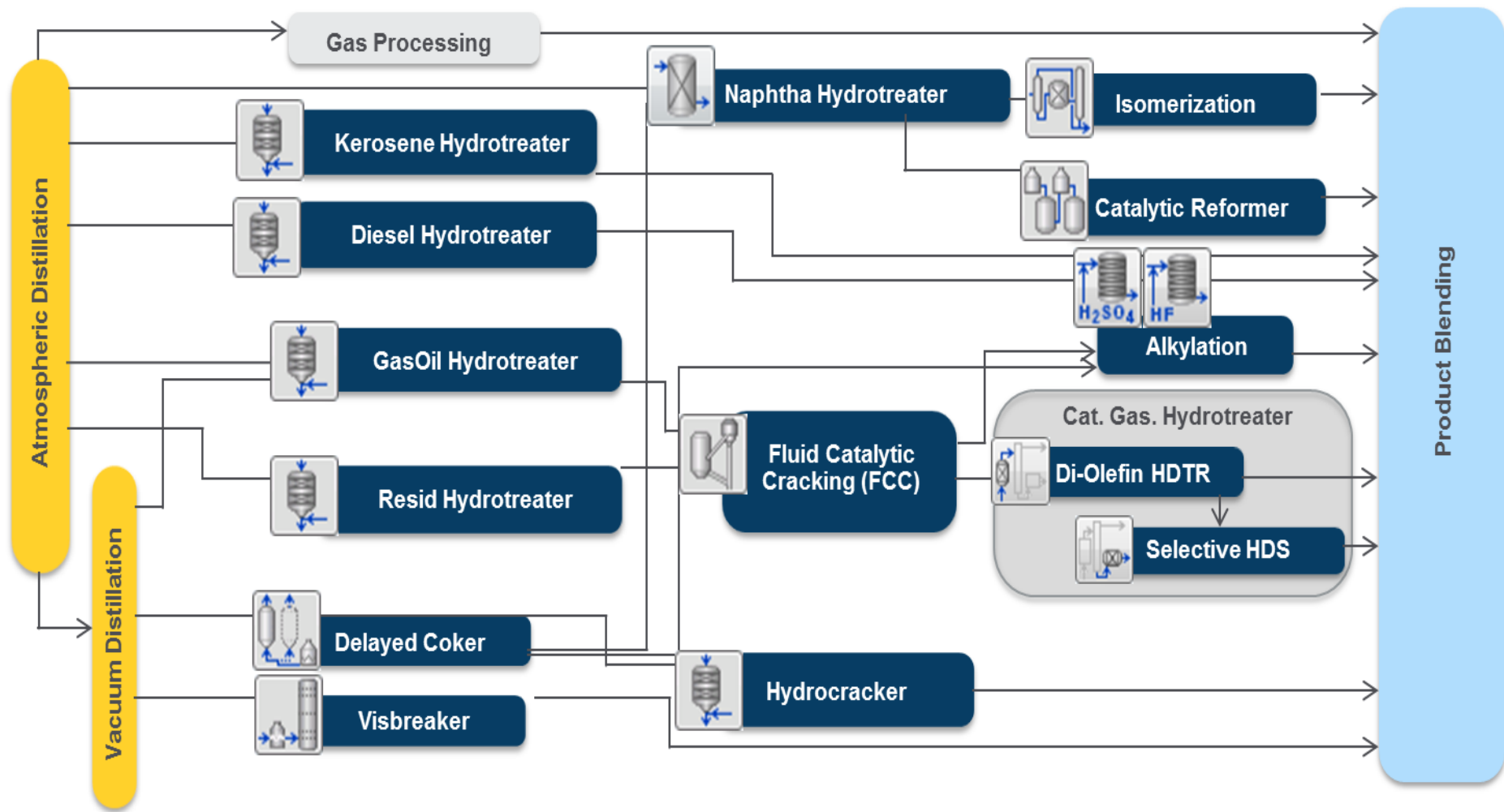


Figure 3.1: Block flow diagram of a Petroleum refinery

Crude distillation process:

Atmospheric distillation is the initial phase of crude oil refining, where crude oil is separated into its fundamental constituents according to their respective boiling points. The process commences with the initial treatment of the crude oil, which involves heating to decrease its thickness and possibly desalination to eliminate contaminants. The heated crude oil is subsequently fed into an atmospheric fractionation column, a long tower that is fitted with trays or packing material. As the crude oil rises up the column, it undergoes vaporization due to the reduction in temperature as it gets higher. As a result of this process, different hydrocarbon fractions in the crude oil condense at their respective temperatures at which they boil. Lighter fractions, such as gasses and gasoline, are collected at higher elevations, while heavier fractions, including diesel and residual oil, condense at lower levels. Heat recovery systems optimize energy utilization throughout the process. The products obtained from air distillation undergo additional processing in subsequent units to manufacture a range of fuels and petrochemicals. On the other hand, vacuum distillation is used to remove the most dense and high-boiling-point components from the atmospheric residue, as they are difficult to separate under normal atmospheric pressure. Vacuum distillation is a process that works at reduced pressures to separate valuable products, such as heavy vacuum gas oil and vacuum residuum. These products have important uses in different industries and can also be utilized as raw materials for other refining operations.

Naphtha catalytic reforming:

Naphtha is a component in crude oil, constituting 15-30wt% and having a boiling temperature range of 30°C-200°C [28]. Catalytic reforming is categorized into three types: semi-regenerative, continuous, and cyclic, based on catalyst regeneration. In the Semi-regenerative process, the operation is continuous, but the catalyst's activity decreases over time due to the decomposition of coke on the catalyst. To maintain the conversion rate, a significant amount of heat is supplied to the process. On the other hand, in the Continuous process, the catalyst is continuously regenerated in a regenerator and then added back into the reactor [29].

Reforming occurs at elevated temperatures (450°C-500°C) and moderate pressures (3-30 bar) in a sequence of reactors, with the presence of hydrogen (3-8 mol H₂ per feed). The feed undergoes first hydro-treatment to eliminate contaminants, such as sulphur, nitrogen, and metal

oxides, that can negatively affect the catalyst. Prior to entering the reactor, the pre-treated feed, along with recycled hydrogen, is heated to a temperature of 498°C. This is where the main reaction, the dehydrogenation of naphtha, takes place. This reaction is endothermic, causing a significant decrease in temperature. To maintain the reaction rate, the gas is heated once again before entering the second reactor. As the reaction progresses, the rate decreases and the reactor becomes larger, requiring less reheat [30].

Hydrotreating:

Hydrotreating is employed to eliminate contaminants, such as heteroatoms (sulphur, nitrogen, and oxygen), as well as metals (vanadium and nickel), from heavy residua. The process occurs at elevated temperatures, usually ranging from 320 °C to 440 °C , in order to reduce cracking. It also operates at high pressure, ranging from 2 to 20 MPa, with a liquid space hour velocity of 0.2 to 8 per hour, and an H₂/oil ratio of 350 to 1800 Nm³/m³. Hydro-treating is conducted in four distinct types of reactors, depending on the catalytic bed used [31], [32].

Prior to entering the reactor, the feed is heated either before or after being mixed with hydrogen gas. The gas is introduced into the reactor from the top, where a reaction occurs between hydrogen gas and liquid residua in the presence of a metal-oxide catalyst. This reaction results in the production of hydrogen sulphide, ammonia, saturated hydrocarbon, and metal. The reaction is exothermic, resulting in a substantial release of energy. Multiple reactors or a single reactor with various catalytic beds and a quench zone in between are employed. The product exits the reactor while the metal remains on the catalyst and is cooled before being introduced into the stripper, where the oil is separated from the hydrogen sulphide and lighter carbon. The oil is sent to the atmospheric fractionator in order to transform it into heavy and light naphtha, medium distillate, and unconverted oil, which is then recycled [30], [33].

The catalyst consumption ranges from 0.003 to 0.02 kg/m³, depending on the intensity of the operation and the amount of metal in the feed. Hydrogen requires around 70 standard cubic feet per barrel of feedstock for every percentage point of sulfur, 320 standard cubic feet per barrel for every percentage point of nitrogen, and 180 standard cubic feet per barrel for every percentage point of oxygen [30].

Isomerization:

This process involves increasing the research octane number of light straight run naphtha while simultaneously reducing the benzene concentration by saturating benzene. The reaction is both reversible and exothermic, occurring at low temperatures due to equilibrium constraints. However, at these low temperatures, the reaction is limited by a slow reaction rate. To enhance the rate, the process primarily relies on the activity and selectivity of the catalyst. Bi-functional catalysts with both acid and metallic sites are employed, selected according to the feed type and working conditions.

The first catalyst is a chlorinated platinum promoted alumina catalyst, which is utilised to enhance the reaction rate at low temperatures (20-130°C) and provide a significant improvement in octane rating (82-84). However, in order to maintain the catalyst's activity, it necessitates the continual addition of organic chloride. Additionally, it is necessary to pre-treat the feed prior to its entry into the reactor due to the catalyst's complete intolerance towards contaminants, which results in catalyst poisoning.

The second option is Pt/zeolite, where platinum is impregnated onto the surface of the zeolite. It functions at elevated temperatures (220-300°C) because to reduced catalyst activity and strong resistance to contaminants, eliminating the need for pre-treatment of the feed. However, it has a low octane rating (76-78). Furthermore, platinum catalysts supported on metal oxide bases have enhanced performance at somewhat elevated temperatures (150°C) and demonstrate excellent resistance to impurities. However, the overall yield of catalysts is very low [34], [35].

Based on configuration, the processes are divided into two categories: once-through and recycling. In the former, unreacted feed is not recycled and the octane number rises from 70 to 82–84, while in the latter, unreacted feed is recycled and the octane number rises to 87–93 [34].

Alkylation:

Olefins such as butene and propane, as well as iso-butane, are utilized as raw materials in the alkylation unit. In this process, they are converted into iso-paraffins, particularly iso-octane. This conversion takes place in the presence of either sulphuric or hydrofluoric acid, which act as catalysts. The purpose of using these catalysts is to minimize undesired side reactions, and this is achieved by maintaining low temperatures (around 50°C) and low pressures (around 30 bar). One advantage of this process is that the resulting iso-octane has a high research octane

number, exceeding 87. Additionally, it has low levels of sulphur and nitrogen content. Alternatively, the conversion can also occur in the absence of a catalyst, but under extreme conditions of high pressure (ranging from 200 to 400 bar) and high temperature (around 500°C). In this case, the resulting iso-octane is considered a blending stock for the green gasoline pool.

Typically, there are two procedures that employ sulphuric acid as a catalyst: auto-refrigeration and effluent refrigeration process. The main distinction between these processes lies in the reactor architecture. In effluent refrigeration, a regeneration unit is used to cool the reactor, whereas in auto refrigeration, the cooling is achieved through the evaporation of iso-butane and propane directly in the reactor. At the process of auto refrigeration, the olefins are introduced into a multi-stage cascade reactor containing an acid catalyst. Butene is also present at each stage, along with a mixer, in order to achieve a high level of reaction selectivity.

The reactor works at a temperature of 5°C and a pressure of 10 pounds per square inch gauge (psig) for a duration of 40 minutes. The gases that evaporate from the reactor are compressed and reintroduced into the reactor together with fresh olefin. Meanwhile, the acid-hydrocarbon emulsion from the previous reactor is cleaned with caustic soda and sent to the de-iso-butanizer, which separates the stream into the desired product. In contrast, effluent refrigeration utilizes a solitary reactor that functions under high pressure of 60 pounds per square inch gauge (psig) and operates at a temperature of 10°C for a duration of 20-25 minutes. Additionally, it incorporates an impeller to improve the mixing of acid and hydrocarbons [36].

In the hydrofluoric acid process, olefins and isobutane undergo dehydration before being combined with hydrofluoric acid in a reactor. The mixing occurs at a specific pressure to ensure that the components remain in the liquid phase. The mixture in the settler separates into two layers, with the acid being collected from the bottom due to its high density. The acid then passes through a chiller to eliminate heat before being recycled. The settler's highest-quality product is sorted into our desired product by running it through a fractionator [30].

Catalytic cracking:

The process of converting heavy oil into a more valuable product is known as cracking. The feedstock for catalytic cracking might consist of air or vacuum residuum, straight run or vacuum gas oil, or a blend of any of these. These feedstocks typically contain a significant

amount of heteroatoms (such as sulphur and nitrogen), asphaltenes, and heavy metals (such as nickel, iron, and vanadium). These impurities can have a detrimental effect on our catalyst, either by poisoning it or reducing its lifespan. Prior to entering the catalytic unit, the feed undergoes pre-treatment, such as hydrotreating or other methods like desulfurization or demetallization. The temperature at which the feed reaches its boiling point falls within the range of 280-540°C [37].

Fluidized catalytic cracking (FCC) is comprised of two main zones: the converter zone and the regenerator zone, with a catalytic stripper located between them [38]. The converter zone, also known as the riser, is made up of interconnected reactors where the hot catalyst comes into contact with pre-treated feed for a very short period of time (less than 5 seconds). In this zone, the heavy oil undergoes cracking. In the regenerator zone, the coke deposits that form on the catalyst as a result of cracking are burned off by passing hot gases at a temperature of 680-710°C. The catalyst is then recycled. The recycled regenerated catalyst generates heat and causes the feed to evaporate at the required reaction temperature of 560 to 580°C. To ensure the productivity of the process, the temperature at the output of the riser is kept within the range of 510-545°C. The catalyst from the riser is sent to the stripper, where a mid-pressure stream is used to remove the light hydrocarbon. Afterward, the catalyst proceeds to the regenerator. The product from the riser is sent to a fractionation column where it is separated into different desired products such as light cycle oil, gasoline, heavy cycle oil, dry gases, and liquefied petroleum gas. Currently, FCC (Fluid Catalytic Cracking) units use FAU-type-Y-zeolite catalysts with an inlet diameter of 0.74nm. These catalysts are preferred because they have higher selectivity and increase the yield of gasoline per conversion [39]

Hydrocracking:

Hydro-cracking is the process of converting heavy oil or vacuum residua into valuable products like gasoline, kerosene, diesel oil, and other light hydrocarbons. This is achieved by reducing contaminants and increasing the ratio of hydrogen to carbon. The reaction occurs in the presence of a hydrogen-rich environment, at a temperature range of 290-400°C, and under a pressure of 8275-13800 kPa. The catalyst commonly employed in hydrocracking consists of silica alumina with a base metal component. This catalyst has a dual purpose: it not only breaks down the heavy hydrocarbon molecules, but also hydrogenates the unsaturated compounds that are either present in the feedstock or generated during the cracking process. The processes that

occur in the hydrocracker can be classified into two groups. The first group involves the hydrogenation of olefins, aromatic rings, sulphur, nitrogen, and oxygen compounds, which is an exothermic process. The second group involves the breaking of carbon-carbon bonds, which is an endothermic process [40]

Various hydrocracking technologies are currently employed to enhance the quality of heavy oil, including fixed bed, ebulliated bed, and slurry bed methods. The choice between a single or multiple stage system in a fixed bed is determined by the feed (middle distillate) and the desired product. The hydro treated feed, along with makeup hydrogen, is heated and then introduced into the reactor. In the case of untreated feed, there is a guard reactor where hydrogenation takes place, converting sulphur and nitrogen into ammonia and hydrogen-sulphide. In the reactor, 40-50 vol% of the feed is cracked, and the resulting effluents are sent to a high pressure separator. In the separator, hydrogen is removed and recycled, while the liquid portion is sent to a fractionation column to be converted into the desired product. The bottom stream from the fractionation column is used as the feed for the second stage, where the unconverted oil is cracked, resulting in a conversion rate of up to 70%. Multiple catalyst beds are employed in conjunction with a cooling stream to regulate and sustain the temperature. The reactor operates in a downhill flow with a temperature range of 530-700 K, a pressure range of 6.5-13.5 MPa, and a mass transfer limiting factor of 1.2-3.0 mm [41]. In the ebulliated bed process, the procedure remains unchanged, except that catalysts are introduced at the top of the reactor along with oil. Hydrogen gas is then bubbled through the mixture, and deactivated catalysts are removed from the bottom. The expansion in catalysts helps to reduce pressure drop and enables the handling of complex feed. The conversion rate of heavy oil in this process is 90%.

In a slurry bed reactor, catalysts in the form of finely distributed (0.002mm) unsupported metal sulfides are utilized to enhance the reaction rate. These catalysts are combined with heavy oil and hydrogen gas before entering the reactor, and are then separated before the product enters the distillation column. Cracking takes place at a temperature range of 400-425°C and a pressure of 16MPa. In addition, achieving uniform mixing at near isothermal conditions enhances the stability and enables a conversion rate of over 90% vol% [42].

Flexi and fluid coking:

This process involves the continuous breakdown of heavy residue from atmospheric and vacuum distillation, as well as the bottom of a catalytic cracking unit and bitumens from oil sand. The aim is to produce lighter products, with a conversion rate of around 70% of the initial feed [43]. In the flexi-coking process, the feed is heated to a temperature of 300°C before being introduced into the reactor. Inside the reactor, it comes into contact with a hot fluidized bed of coke, which is maintained at a temperature ranging from 480°C to 550°C. This high temperature provides the necessary heat for the occurrence of the endothermic reaction. The coke undergoes recycling from the reactor to the heater, which operates at a temperature of 624°C. During this process, the coke particles are burned through partial combustion. A fraction of coke is recycled from the heater to the gasifier, which operates at a temperature of 1000°C. This process converts any extra coke into flue gas. Additionally, some gas from the top of the gasifier and unconverted coke from the bottom are sent back to the heater. The purpose of this is to give the necessary energy to burn the coke. The cracked product generated in the reactor is sent through a cyclone separator positioned at the top of the reactor. This separator effectively separates coke particles from the product. The separated product then proceeds to a scrubber, where it is rapidly cooled and sent to a fractionator for further separation. Scrubbers utilize wash oils for the purpose of condensation.

A portion of the high boiling cracked vapor (+495°C) is condensed and returned to the reactor for recycling. The coke generated during the cracking process is removed by means of a stream at the bottom of the reactor in order to avoid the cracking products from being contaminated with the coke that remains in the reactor. The coke gas exiting the heater undergoes cyclone separation and heat recovery prior to entering the scrubber and sulphur removal system. The pure gas that exits has a modest heating value of 100 BTU, which is utilized for the generation of steam and electricity. Fluid coking, also known as flexi coking, is a process where the heater is substituted with a burner and no gasifier is utilized. This method results in the production of a significant volume of coke, of which around 20-25% is combusted using air and heat [44].

Delayed coking:

A thermal conversion technique is employed to enhance the heavy residue into the required product. This process can handle a wide range of feedstock and produce a metal and carbon-free product through partial conversion into a liquid product. However, it also generates a

significant amount of coke, ranging from 20-30%, resulting in low yield and a strongly aromatic product. Consequently, this process is quite expensive. The selectivity of the process is contingent upon the working conditions, such as temperature and pressure [43]. The process comprises two coke drums, a furnace, and a fractionator. The incoming feed is heated to a temperature of 350°C through heat exchange with hot gas oil product or, in rare instances, by passing through a furnace. It enters the fractionator at the bottom and is mixed with a small percentage (between 2-3%) of heavier end material recycled from the fractionator. Next, the mixture is sent into a furnace where it is heated to a temperature of 500°C and subjected to a pressure of 4 bar. Steam is introduced to enhance the flow velocity and inhibit coking reactions in the furnace [45].

After undergoing partial vaporization and being introduced into the coke drum, the feed undergoes a reaction. The drum is then insulated for a period of 16-18 hours and thereafter filled. High-pressure water is injected to remove coke deposits from the walls of the heating tubes. The reactors operate alternately in a 24-hour execution cycle in batch mode. When one reactor is operating, the other is decoked or cleaned by putting steam into the coker drum to remove hydrocarbon vapors. The drum is then cooled by filling it with water and draining it, after which the coke is removed. The high-temperature gases emitted by the coking drum are introduced into the fractionating column, namely 2-3 plates above the bottom. These gases are then separated based on their boiling points, resulting in the extraction of various substances such as naphtha, wet gas oil, light gas oil, and heavy gas oil. The plates of the fractionator undergo a washing process to eliminate the accumulation of coke deposits on plate [46], [47].

Table 3.1: Time span of operations occurring in Delayed Coking Unit

Operation	Hours
Fill drum with coke	24
Switch and steam out	3
Cool	3
Drain	2
Unhead and decoked	5

3.2 Exergy analysis formulation

Exergy analysis utilizes the principles of the first and second laws of thermodynamics to assess the energy conservation possibilities of a system. The term "maximum useful work" refers to the highest amount of work that a reversible system can create while it is in thermodynamic equilibrium with its surrounding environment [48]. In equation (3.1), the system's exergy is composed of both chemical exergy and physical exergy.

$$Ex_{sys} = Ex_{ph} + Ex_{che} \quad (3.1)$$

Physical exergy (Ex_{ph}) refers to the highest amount of usable work that a system can generate when it is transitioned from its initial state to the environmental state (T_0, P_0), as indicated by equation (3.2).

$$Ex_{ph} = \dot{m}[(h - h_0) - T_0(s - s_0)] \quad (3.2)$$

The symbols \dot{m} , h , and s represent the mass flowrate, enthalpy, and entropy at the current operating conditions. On the other hand, h_0 and s_0 represent the enthalpy and entropy at standard conditions.

Chemical exergy (Ex_{che}) refers to the highest amount of useful work that a system can generate when it is transitioned from its initial environmental state to a state of complete equilibrium, as represented by equation (3.3).

$$Ex_{che} = \dot{m} \left[\sum_{i=1}^n X_i (e_i X_i) \right] \quad (3.3)$$

X_i represents the mole fraction, while $e_i X_i$ represents the typical chemical exergy of a substance, which is computed using equation (3.4). The symbol $g_{f,i}$ represents the standard molar free energy of formation, while $e_j X_j$ represents the molar standard chemical exergy of each constituent element [49], [50]

$$e_i^0 = g_{f,i} + \sum_{j=1}^{n,i} X_j (e_j X_j) \quad (3.4)$$

3.2.1 Exergy performance indicator

The exergy analysis is conducted to determine the system's thermodynamic efficiency. The system consists of three components: system exergy efficiency, exergetic improvement potential, and irreversibility.

Irreversibility or exergy destruction:

This measures the quantity of exergy that is lost or wasted throughout the unit process. Put simply, it pertains to the variance between the exergy entering and leaving a unit process as determined by equation (3.5).

$$I = Ex_{destroyed} = \sum Ex_{in} - \sum Ex_{out} \quad (3.5)$$

Certain process equipments, such as distillation columns, the condensation unit and the reboiler play a crucial role to ensure that the energy balance is maintained in addition to the INPUT streams (feed) and OUTPUT streams (product), the computation of irreversibilities is adjusted by modifying the equation (3.5) to (3.6).

$$I = \sum (\dot{E}x_{feed} + (1 - \frac{T_o}{T_r})Q_r) - \sum (\dot{E}x_{product} + (1 - \frac{T_o}{T_c})Q_c) \quad (3.6)$$

Q_r and Q_c represent the heat duty of the reboiler and condenser, respectively. T_r and T_c indicate the temperature of the reboiler and condenser.

Exergetic improvement potential:

The term refers to the quantification of the extent to which irreversibility can be minimized in a single procedure. The abbreviation 'I.P' represents the term and it is mathematically represented by equation (3.7).

$$IP = (1 - \eta)(E_{in} - E_{out}) \quad (3.7)$$

Exergy efficiency:

Evaluates the effectiveness of the system in comparison to its performance. In simple terms, it is the proportion of output to input exergy, which can be determined using equation (3.8) [51].

$$\varphi_{universal} = \frac{E_{out}}{E_{in}} \times 100 \quad (3.8)$$

3.3 Artificial neural network (ANN)

Artificial neural networks (ANNs) are a dynamic machine learning methodology that draws inspiration from the intricate structure and functioning of the human brain. Artificial neural networks (ANNs) consist of interconnected nodes, like the neurons seen in a real brain. These networks have the ability to learn and execute intricate tasks by processing and analysing vast quantities of data. One of the primary advantages of artificial neural networks (ANNs) is their capacity for parallel processing, enabling them to do numerous tasks concurrently. Additionally, they possess the capability to store information throughout the entire network, as opposed to a centralised database, which enhances their fault-tolerance and resilience against data loss. Artificial neural networks (ANNs) are highly proficient in describing intricate and non-linear connections between input and output variables. This ability is essential for correctly depicting real-world events.

Artificial neural networks (ANN) use learning and training to quantitatively analyse data [52]. Interconnected nodes, or "neurons," stacked in layers. ANNs are trained by changing synaptic weights to reduce errors and improve prediction and decision-making. Neurons process inputs and outputs using their activation function. Different weights are assigned to each input.

Figure 3.2 shows that the neuron's output is influenced by a non-linear relationship between its inputs (x_1, x_2, \dots, x_m) and their weights ($w_{k1}, w_{k2}, \dots, w_{km}$). Synaptic weights are adjusted during learning to fine-tune the network. This learning method uses a dataset with fixed input and output values. Figure 3.2 shows bias as 'b_k' and activation function as 'φ'.

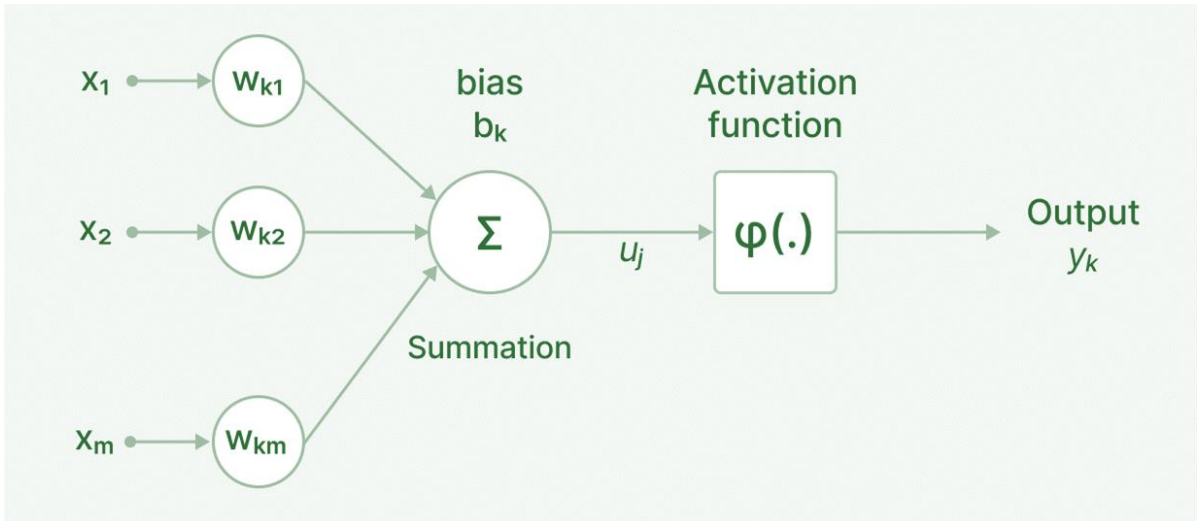


Figure 3.2: Structure of neuron

A typical network has three layers: input, hidden, and output. As shown in Figure 3.3, these layers store complex, non-linear functions. Input's layer purpose is to receive external data, features, and information. Hidden layer neurons extract system-relevant data. Neurons at the output layer generate and send network outputs. The outputs are a consequence of the computations performed by the neurons in the preceding layer.

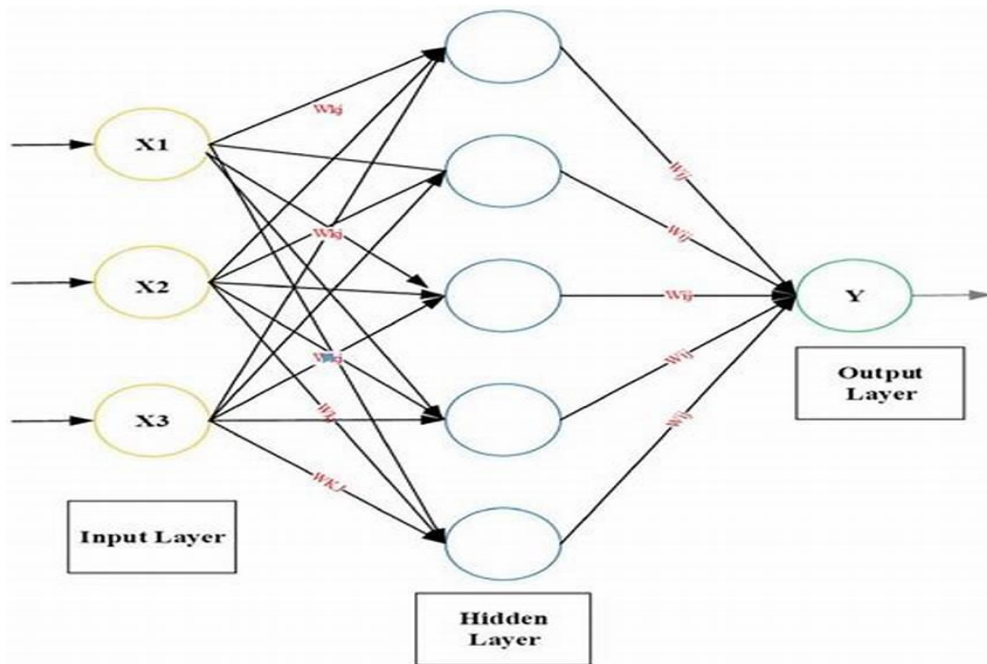


Figure 3.3: Structure of Artificial Neural Network (ANN)

Although artificial neural networks (ANNs) offer numerous advantages, they also possess certain limits. Their opaque character, in which the core mechanisms of the network are not readily understandable, can provide difficulties in specific applications where transparency and comprehensibility are essential. The current research is focused on tackling these difficulties and broadening the range of Artificial Neural Network (ANN) applications in other fields.

This study utilised a MATLAB-based artificial neural network (ANN) tool to streamline the optimisation process. MATLAB, a robust programming language and software development environment, is highly suitable for developing artificial neural networks (ANNs) because of its comprehensive capabilities and specialised functions designed for the purpose of designing and training neural networks. By making this approach, the researchers were able to have a broad selection of tools and features at their disposal to optimise the artificial neural network architecture and efficiently manage intricate datasets.

Using MATLAB for ANN creation offers numerous benefits that go beyond its diverse capabilities. The platform's extensive visualisation tools were essential in facilitating the debugging and analysis of the artificial neural network's performance. Researchers can get significant insights into the learning process and identify potential flaws or areas of development by visualising the network's topology, weight distributions, and activation patterns during training.

Furthermore, the user-friendly interface and easy programming syntax of MATLAB facilitated a smooth integration of the ANN into the research workflow. The researchers were able to prioritise the optimisation process and experimentation due to the user-friendly nature and concise syntax, without being hindered by intricate implementation details. Efficient and effective solutions were accomplished by utilising MATLAB's capabilities for developing and optimising artificial neural networks (ANNs). The integration of MATLAB's comprehensive features, visualisation capabilities, and intuitive interface facilitated an efficient and fruitful research workflow. Consequently, the study produced an efficiently optimised artificial neural network (ANN) model that can accurately predict and extract valuable insights from the intricate dataset. This further highlights the importance of utilising MATLAB as a valuable tool in the realm of artificial neural networks and machine learning research.

3.3.1 The LM method

The Levenberg-Marquardt approach is utilised to solve the nonlinear programming problem by iteratively updating a set of parameters by a combination of gradient descent and Gauss-Newton updates. The objective is to minimise the sum of squared errors between the model function and the given data points, as represented by equation (3.9).

$$[J^T W J + \lambda(J^T W J)]h_{lm} = J^T W(y - \hat{y}) \quad (3.9)$$

The gradient descent method minimises the sum of squared errors by adjusting the parameters in the direction of steepest descent. The Gauss-Newton method decreases the sum of the squared errors by assuming that the least squares function is locally quadratic in the parameters and finding the minimum of this quadratic. The update is called a gradient descent update if the dumping parameter λ is big, and a Gauss-Newton update if it is too small. In order for the initial updates to be brief steps in the steepest-descent direction, the damping variable λ is initially set to a large value. As the answer got better and the algorithm got closer to the Gauss-Newton method, the λ got smaller and less until it eventually settled on a local minimum [53].

3.3.2 The scaled conjugate method

The scaled conjugate technique is a mathematical optimisation approach employed to determine the global minimum of a given function. It is a modified version of the conjugate gradient method, which is a widely used approach for addressing optimisation issues on a large scale. The scaled conjugate approach, created by Martin Møller in 1993, is renowned for its high efficiency and resilience.

The fundamental concept underlying the scaled conjugate technique is to merge the benefits of the conjugate gradient approach with a scaling mechanism that enhances the rate at which convergence occurs. The approach operates by iteratively modifying the search direction and step size, utilising knowledge of the gradient and Hessian (the matrix of second-order partial derivatives) of the function.

The algorithm commences by setting the search direction and the step size to their initial values. During each iteration, the approach calculates the gradient and Hessian of the function at the current point. It then utilises this information to modify the search direction and step size. The

update rules are formulated to maintain the conjugacy of the search direction with the preceding search directions, hence facilitating the acceleration of convergence.

An important benefit of the scaled conjugate method is its avoidance of the need to explicitly calculate the Hessian matrix, which can be computationally burdensome for situations of significant scale. Alternatively, the approach employs a scaling mechanism to estimate the Hessian, hence decreasing the computing expense and enhancing the method's efficiency.

In this research study “The Scaled Conjugate method” is used.

3.4 Genetic algorithm (GA)

A genetic algorithm is an effective optimisation methodology that draws inspiration from the principles of natural selection and genetics. The system functions by iteratively generating and refining a set of potential solutions to a given problem, emulating the mechanisms of genetic inheritance, mutation, and selection, as depicted in Figure 3.4. Through a process known as natural selection, people that possess advantageous features or characteristics have a higher probability of being selected to reproduce in each generation. This gradual selection process leads to an improvement in the quality of solutions to the problem over time [54].

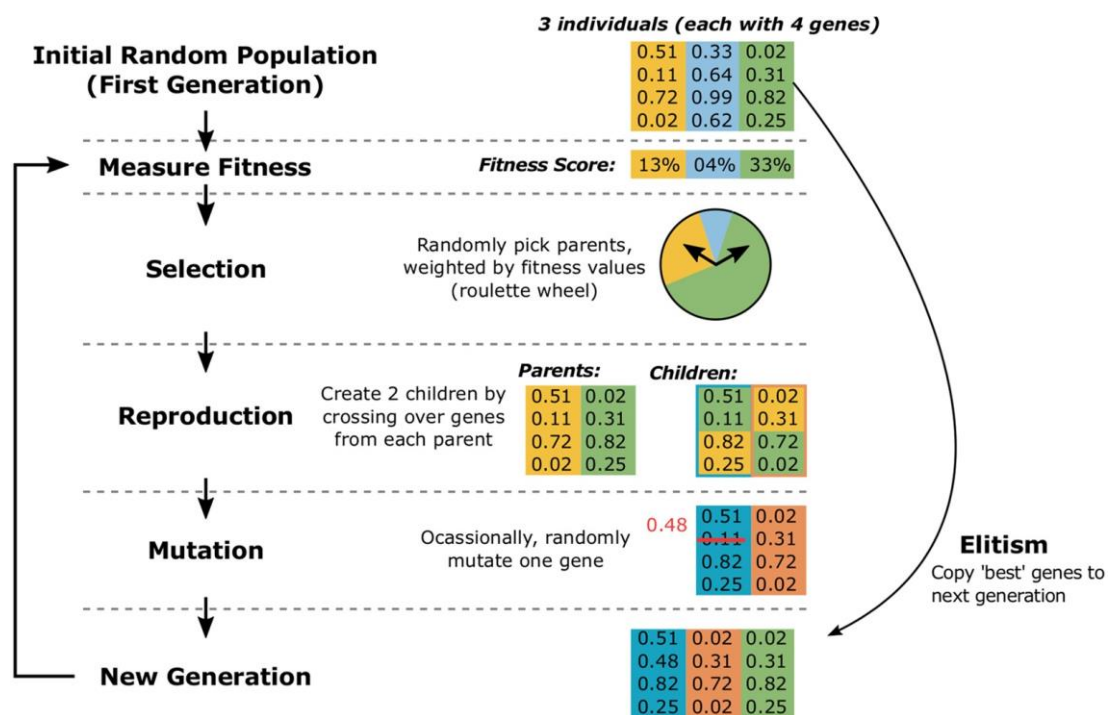


Figure 3.4: Schematic representation of Genetic Algorithm [29]

3.4.1 Genetic operations

Each genetic operator serves the following purposes.

Population:

A random sample of the population was initially formed. Each potential solution is referred to as a chromosome, as seen in Table 3.2.

$$P = \{p_1, p_2, \dots, p_{pop_size}\} \quad (3.10)$$

$$p_i = [p_{i_1} p_{i_2} \dots p_{i_j} \dots p_{i_{no_vars}}] \quad (3.11)$$

$$para_{min}^j \leq p_{i_j} \leq para_{max}^j \quad (3.12)$$

Table 3.2: Chromosomes

Chromosome 1	1101100100110110
Chromosome 2	1101111000011110

In equation 3.10, the term "pop_size" represents the overall size of the population. In equation 3.11, the term "no_vars" represents the number of variables that need to be adjusted. The terms " $para_{min}^j$ " and " $para_{max}^j$ " refer to the minimum and maximum values of the parameter p_{i_j} .

Selection:

During each succeeding generation, choose a subset of the current population to reproduce and create a new population. Individual solutions are chosen using fitness-based approaches. The feasibility of each proposal is assessed, and the most advantageous one is chosen. The selection methods of roulette wheel, rank, stochastic universal sampling, and tournaments are widely recognized [55].

Roulette wheel selection involves mapping potential strings onto a wheel and allocating a portion of the wheel based on its fitness value. Subsequently, the wheel undergoes a random rotation to determine specific solutions that will contribute to the creation of the subsequent

generation, as depicted in Figure 3.5. The rank selection method has been enhanced from the previous roulette wheel approach. Individuals are assessed according to their rankings rather than their fitness worth, providing each individual with an opportunity to be chosen.

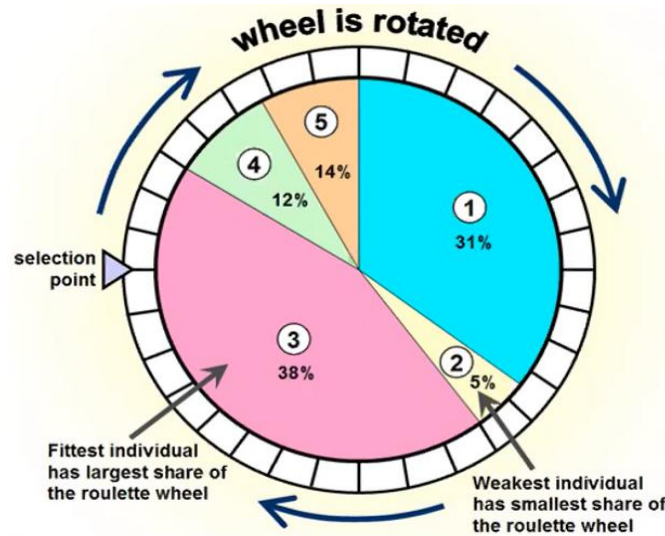


Figure 3.5: Roulette wheel selection

Stochastic universal sampling (SUS) chooses a new individual from a generation by evenly spacing the intervals and starting at a random point in a list of individuals. The system provides equitable opportunities for every applicant to be selected.

Tournament selection is used to choose individuals based on their fitness value. This selection process involves a stochastic roulette wheel. The fittest individual is selected and included in the pool of the succeeding generation, as seen in Figure 3.6 [56]

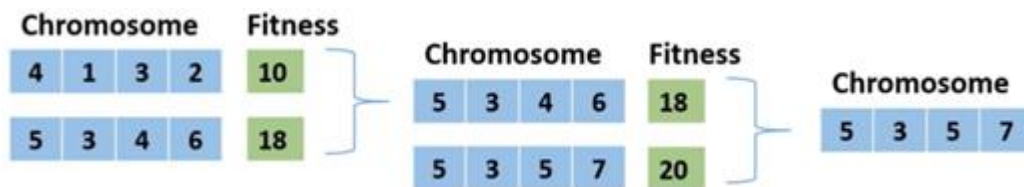


Figure 3.6: Selection of the Tournament

Crossover.

Offspring are generated by merging the genetic material of two parents from the preceding generation.

A single-point crossover involves selecting a random point and exchanging genetic information between the parents beyond that point, as seen in Figure 3.7

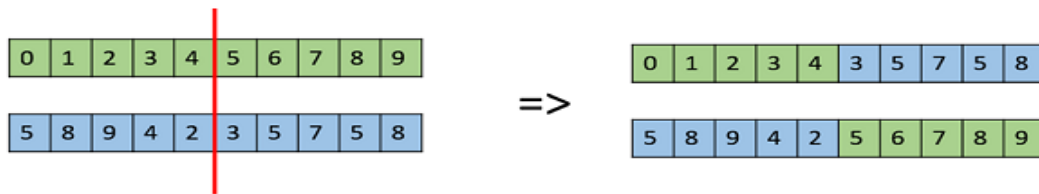


Figure 3.7: Single point cross over

Double point crossover involves the random selection of two sites. At these locations, genetic information is exchanged between both parents, as seen in Figure 3.8



Figure 3.8: Double point crossover

The uniform crossover treats each gene in the parents as separate entities. The decision to exchange the gene for a distinct chromosome at the corresponding place is made arbitrarily, as depicted in Figure 3.9.

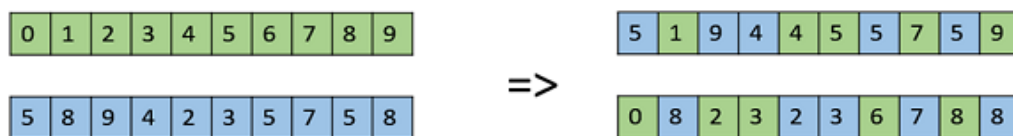


Figure 3.9: Uniform crossover

During the process of dispersed crossover, a random chromosome is formed and genes are picked based on whether a chromosome is 0 from the second parent or 1 from the first parent. Subsequently, both entities are merged to create a progeny.

Mutation:

Preserves the genetic variety between successive populations. Genes within the chromosomes undergo alterations throughout the process of mutation. Consequently, the traits of

chromosomes inherited from parents may undergo modifications. The mutation technique will generate three extra offspring [55].

3.5 Particelle swarm optimization (PSO)

Eberhart and Kennedy originally developed particle swarm optimization, which is an evolutionary approach to optimisation that is chaotic and population-based [57]. The primary idea behind the PSO algorithm is to guide the swarm by using information exchanged between the particles to arrive at the optimal position. Every particle and every bird in the search space has a unique position and velocity. A particle's best position (P_{best}) is established by taking into account both its previous velocity and the best location discovered by its nearby particles. G_{best} is the total best position among all of the particles. While G_{best} is influenced by the collective experiences of nearby particles in the swarm, P_{best} is decided by the ideal experience of a single particle. Until a predefined stopping threshold is reached, the algorithm constantly computes the updated velocities and positions of the particles by changing the velocity location and neighbours. Each particle has two characteristics: its position and velocity, which are vectors in an n-dimensional space. The link between the particle's position and the amount of mobility dictates how the particles and swarm. Equations 3.16 and 3.17 can be used to find the position and velocity of any given particle.

$$V_{i+1} = WV_i + C_1r_1(P_{best}-X_i) + C_2r_2(G_{best}-X_i) \quad (3.16)$$

$$X_{i+1} = X_i + V_{i+1} \quad (3.17)$$

In equations 3.16 and 3.17, the variable P_{best} represents the optimal position of the ith particle, while G_{best} represents the optimal position among all particles. V_i represents the velocity of the ith particle, X_i denotes the position of the particle, W represents the inertial weight; C_1 and C_2 are acceleration factors that influence the convergence of optimization. r_1 and r_2 are random variables uniformly distributed in the interval $[0,1]$. The Figure 3.10 presents the flowchart of particle swarm optimization.

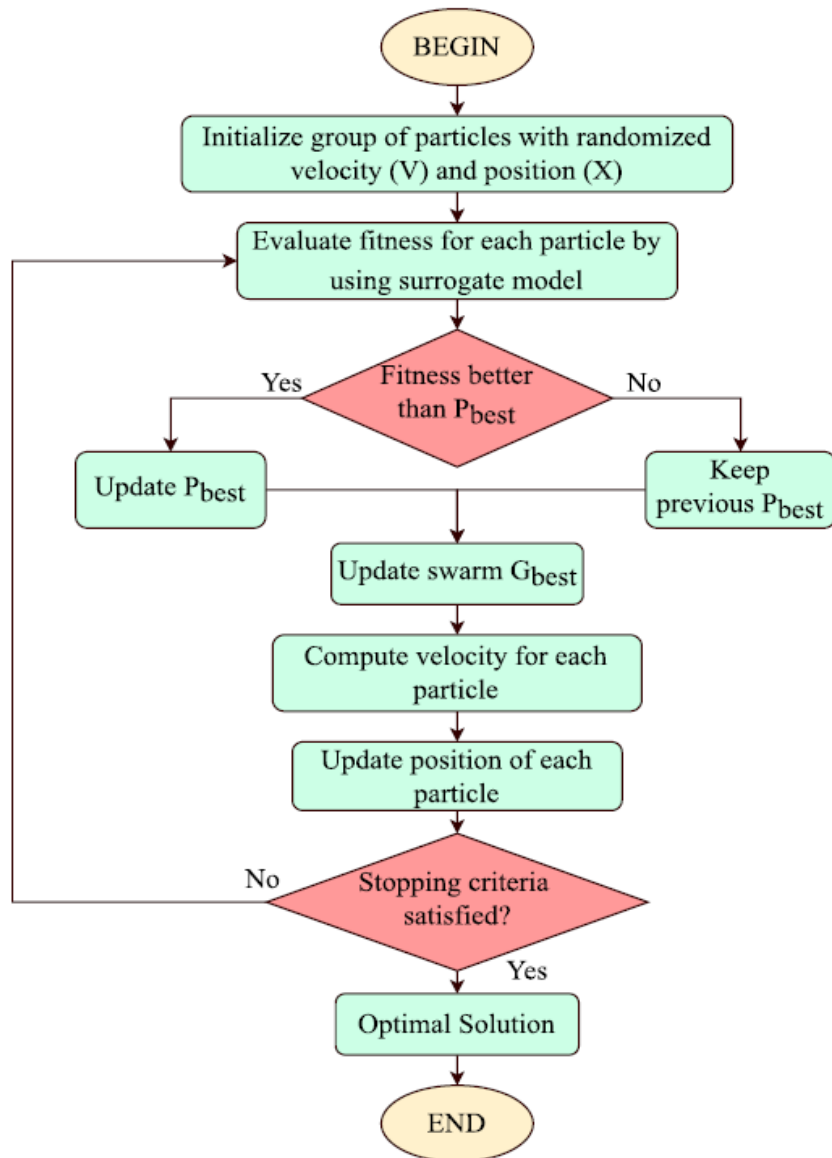


Figure 3.10: Flowchart of particle swarm optimization

3.6 Methodology

A summary of the study's methodology is provided in Figure 3.11. The five main steps of the approach are briefly summarised below:

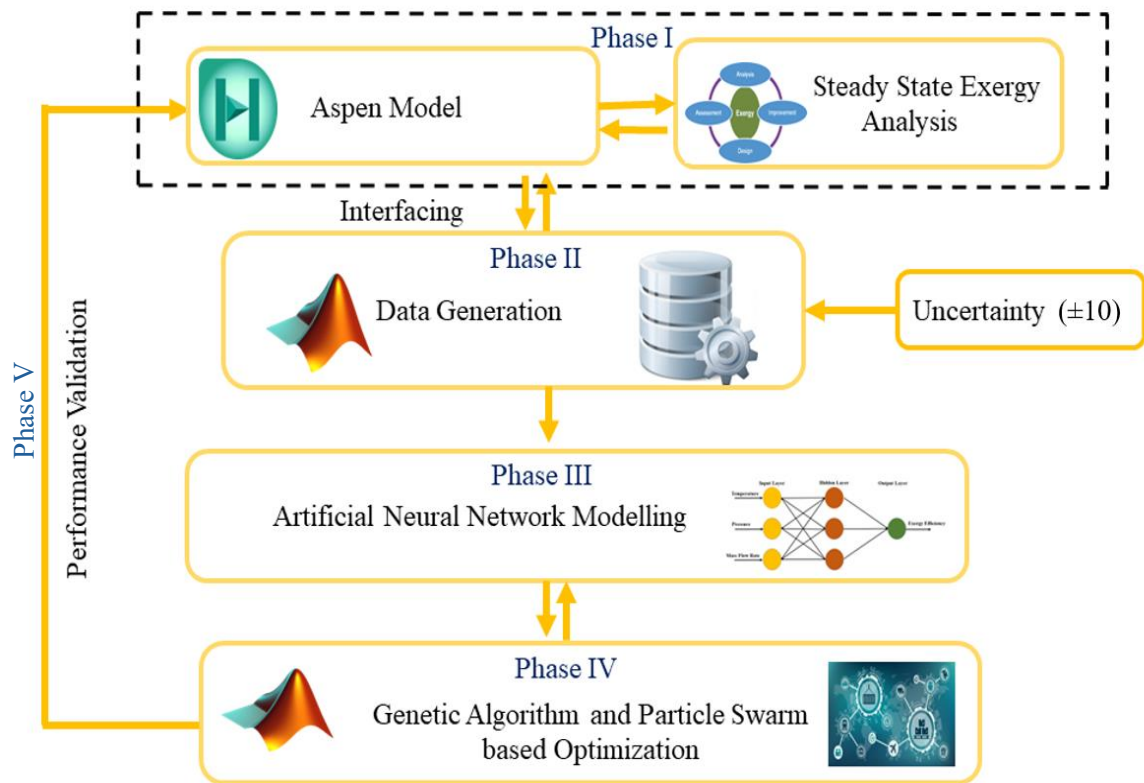


Figure 3.11: Methodology

Phase I: Steady-state exergy analysis

Following assumptions were made during exergy analysis.

- Process units were modelled and evaluated as a steady-state flow system.
- Potential and kinetic exergies were ignored.

The physical exergy of the process was calculated from the Aspen HYSYS V.11 property set. Then using the values of exergy the process irreversibility or exergy destruction and exergy efficiency were calculated using equations (3.5) and (3.8). Exergetic improvement potential of the process and equipment were calculated using the values of exergy destruction and efficiency from using equation (3.7).

Phase II: Data generation

Through COM server an interface was created between Aspen HYSYS and MATLAB software to generate data samples from the selected degree of freedom. The data sets were generated under random -10% and +10% uncertainty in process parameters. A total of 500 data samples were generated. Overall plant exergy efficiency was calculated for each data samples.

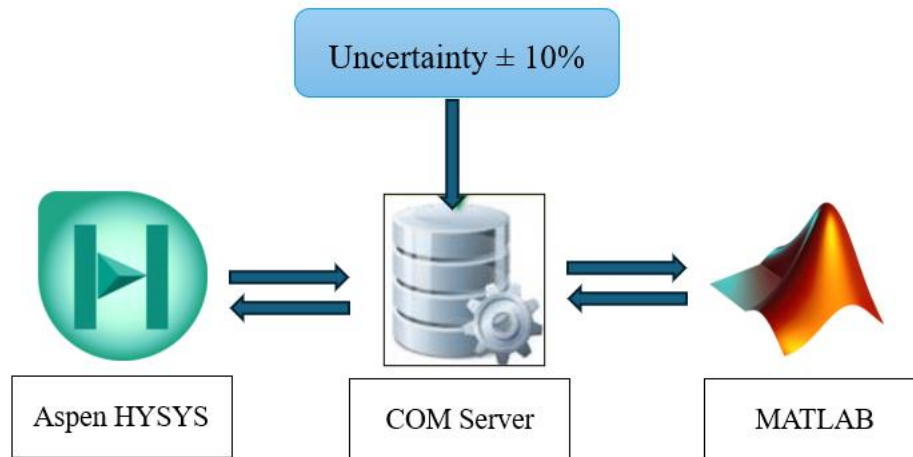


Figure 3.12: Data generation under uncertainty

Then the manipulated variables of these streams, such as temperature, pressure, and mass flow rates were calculated repeatedly via MATLAB, and about 500 data sets were generated, and so as the exergy efficiency, exergy destruction, and exergetic improvement potential for each case.

Phase III: ANN modeling

An ANN model was developed and validated using MATLAB 2021a. The modeling consists of model selection, training and validation.

- **Model selection:** A feed-forward neural network was selected with the Scaled Conjugate (trainscg) backpropagation training algorithm. Eighty percent (80%) of the data set is used for training; the rest of data samples are divided equally for model validation and testing. In this case, the ANN model has 36 input neurons, 3 hidden layers (containing 60 neurons in 1st hidden layer, 50 neurons in 2nd hidden layer, and 40 neurons in 3rd hidden layer) and 1 output neurons. The process exergy efficiency is represented by the output neuron, while the unpredictable process situation is represented by the input neuron. The number of hidden layers and neurons within each hidden layer were chosen via trial and error. The ANN was programmed to operate with a minimum gradient of 1e-5 for 1000 epochs.

- **Training and validation:** The model is validated by following two criteria
 - Root mean-squared error (RMSE) and
 - Relation coefficient

RMSE is calculated from equation (3.13) and R from equation (3.14).

$$RMSE = \sqrt{\frac{1}{n} \sum_{i=0}^n (Y_i^{exp} - Y_i)^2} \quad (3.13)$$

$$R = 1 - \left[\frac{\sum_{i=0}^n (Y_i^{exp} - Y_i)}{\sum_{i=0}^n (Y_i^{exp} - Y_{avg})} \right] \quad (3.14)$$

Y_i^{exp} represents the experimental value, Y_i represents the anticipated data, and n is the number of test samples. Root Mean Square Error (RMSE) is a value that is always greater than or equal to zero, and a smaller value indicates a higher level of accuracy in the model's predictions. The coefficient of determination, often known as R-squared, is a statistical measure that quantifies the proportion of the variance in the response variable that can be explained by the regressor variables. It ranges from 0 to 1, with 0 indicating that the output variable cannot be anticipated from the regressor variable, and 1 indicating that the response variable can be fully predicted from the regressor variables.

Phase IV: Optimization:

An Artificial Neural Network (ANN) model was employed as a substitute in a Genetic Algorithm (GA) and Particle Swarm Optimization (PSO) setting to optimize a system under unknown conditions, with the purpose of maximizing exergy efficiency. The Genetic Algorithm (GA) and Particle Swarm Optimization (PSO) successfully determined the ideal parameter that maximizes exergy efficiency.

The algorithm steps for the Genetic Algorithm (GA) are as follows:

- 1) The procedure begins by generating a set of randomly selected populations of individual solutions.

- 2) Conducted a fitness assessment of each member in the population using a surrogate model and ranked them based on their fitness value.
- 3) Parents are picked based on their fitness value to create offspring utilizing the crossover operator.
- 4) Mutation operators are employed to improve the quality and preserve the genetic variety of the subsequent generation.
- 5) The algorithm terminates if the criteria of the objective function are satisfied; otherwise, steps 2-4 are repeated until an optimal solution is achieved.

The procedure for the Particle Swarm Optimization (PSO) algorithm is as follows:

- 1) The method commences by creating initial particles and assigning them an initial velocity.
- 2) A surrogate model was employed to assess the position of the particle.
- 3) If the current position is superior to the old one, update the new personal best.
- 4) Set the global best value to the new personal best.
- 5) Determine the new particle velocity by considering the present velocity and the optimal positions of both the particular particle and its neighboring particles.
- 6) Continue doing steps 2-5 until the halting requirement is met.

The efficacy of the proposed optimization was confirmed by executing the Aspen HYSYS model on the optimized outcomes and determining the absolute discrepancy.

Phase-V: Results validation

Values predicted and optimized by GA and PSO were then fed into the Aspen HYSYS first principle model to validate the results.

CHAPTER 04: RESULTS AND DISCUSSION

Section 4.1 presents the steady state exergy analysis of petroleum refinery process, while Section 4.2 presents the data-based modeling and optimization of exergy efficiency.

4.1 Steady state exergy analysis of petroleum refinery

This section includes the steady state exergy analysis of petroleum refinery process which was modeled in ASPEN HYSYS. Details are given in the following section.

4.1.1 Stream wise exergy analysis

From the simulated petroleum refinery model, the process information was extracted in ASPEN Spreadsheet. By the help of the extracted data the physical exergies of each stream is calculated which is shown in Table 4.1. This table outlines the physical exergy values of various streams in a refinery are measured in kilojoules per second (kJ/s). Each row represents a different stream, such as steam from different Crude Distillation Units (CDUs), and input streams. Moreover, it includes utility streams, primarily hydrogen used in various processes. The total physical exergy entering the system sums up to 26,235.92 kJ/s, reflecting the aggregate energy potential of all streams involved. This information is important for analyzing and optimizing the energy efficiency and resource utilization of the plant.

Table 4.1: Input streams physical exergies

S.no	Stream names	Physical exergy (kJ/s)
1	Main Stream CDU1	589.51
2	Kero_SS_Stream COL3	39.50
3	Diesel Steam CDU1	157.20
4	Vac Steam CDU1	196.50
5	Etame CDU1	179.18
6	Rabi Blend CDU1	106.98
7	Main Steam CDU2	1965.02
8	Kero_SS_Steam Col5	197.50
9	Diesel SteamCDU2	294.75
10	Vac STeam CDU2	196.50
11	Arab Heavy CDU2	226.08
12	BCF-17 CDU2	5.58
13	Dalia CDU2	172.15
14	Marlim CDU2	151.59
15	RGN @CDU2	17.53
16	Main Steam CDU3	196.50

17	Kero_SS_Steam Coll	98.75
18	Diesel SteamCDU3	78.60
19	Vac STeam CDU3	49.13
20	Arab Light CDU3	138.21
21	ALK1 @TPL13	2.22
22	NC4 @TPL13	43.56
23	C3 from Dimerisation @TPL16	65.38
24	Dimate Stream @TPL16	0.74
25	HCK Copy @TPL 19	82.20
26	KHT Copy @ TPL19	1281.02
27	Purchased Heavy Naptha	215.10
28	Ethanol Purchase	228.67
29	NC4 Purchase	1.34
30	H2 fot NHT @TPL29	345.79
31	H2 for KHT @TPL31	152.52
32	H2 for DHT @TPL 33	836.67
33	H2 for GOHT @TPL34	4350.58
34	H2 for HCU @TPL36	12542.08
35	LCN Properties @TPL37	782.96
36	H2 for C5 Isom @TPL38	20.64
37	H2 for Scanfiner @TPL39	224.80
38	H2 for C4 Isom @TPL40	2.88
	Total Physical Exergy IN	26235.92

Out of these 38 input streams, following are the streams with low amount of physical exergies, as shown in figure 4.1.

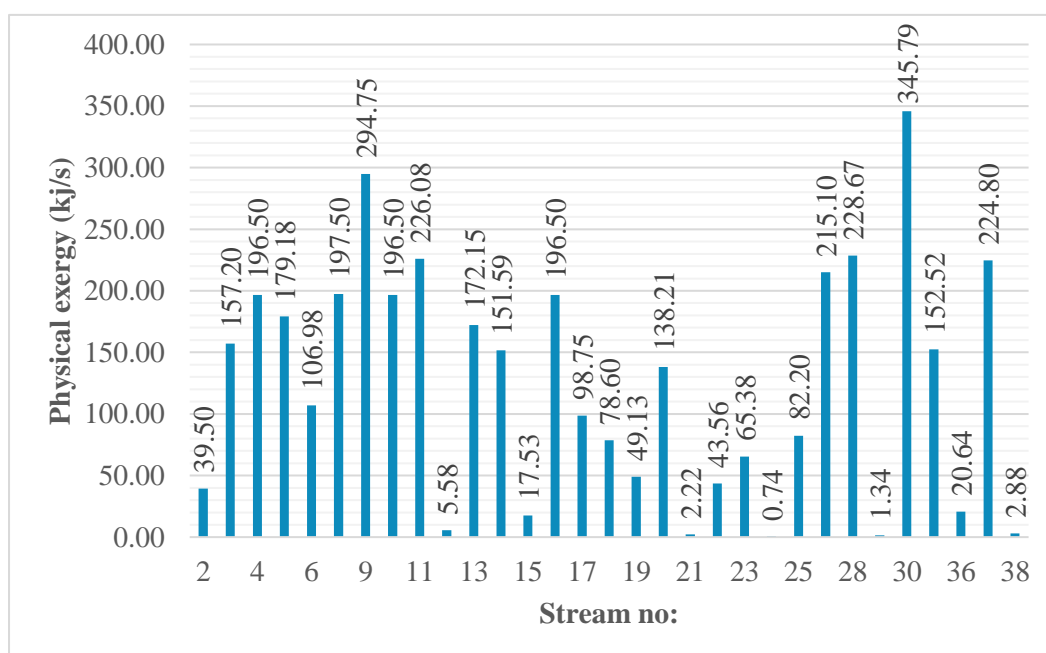


Figure 4.1: Input streams with low physical exergies

The remaining streams which have the highest amount of exergy are shown graphically in the following figure 4.2.

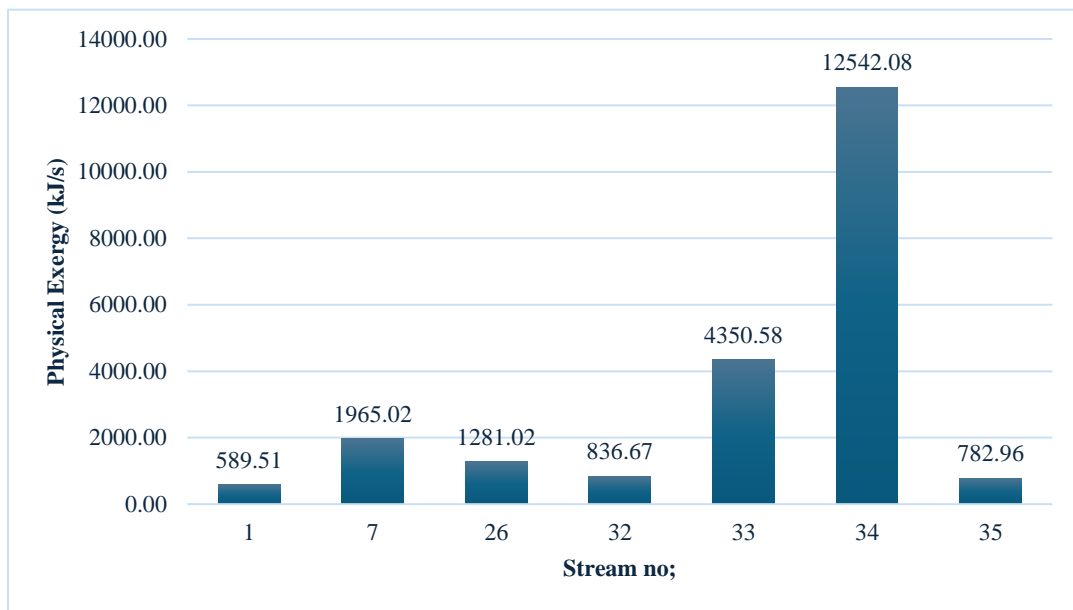


Figure 4.2: Input Streams with high physical exergies

The same is for output streams, by the help of the extracted data the physical exergies of each stream is calculated as shown in Table 4.2. This table lists the physical exergy of various output streams from a processing facility, measured in kilojoules per second (kJ/s). It includes a wide range of streams such as sour water, various off-gases, and several product categories like jet/kero, diesel, and different grades of gasoline. High exergy values are noted for products like conventional premium gasoline (2,985.70 kJ/s), jet/kero copy (1,340.30 kJ/s), and reformulated regular gasoline (677.44 kJ/s). Moreover, significant exergy is associated with hydrogen streams from various processes, including ARF Hydrogen (2,265.44 kJ/s) and H₂ from Gasolene Reformer (1,214.61 kJ/s). The total physical exergy of all output streams sums up to 18,923.94 kJ/s, representing the cumulative exergy available from the facility's outputs.

Table 4.2: Output streams physical exergies

S.No	Stream Names	Physical Exergy (kJ/s)
1	Sour Water	12.16
2	Vac Ovhd 1	25.27
3	NC3 CD1	1.78
4	offgas cd1	0.06
5	Sour Water	28.27
6	Vac Ovhd 2	183.26
7	NC3 CD2	7.99
8	Offgas CD2	0.14
9	Sour Water	3.32

10	Vac Ovhd 3	29.56
11	NC3 CD3	2.16
12	OFF GAS CD3	0.04
13	NC4 floating	10.77
14	iC4 Floating	2.37
15	iC4 to SSFA	63.18
16	C4X	123.83
17	C4M	530.68
18	C3M	342.14
19	C3X	110.41
20	C3 from Dimerisation	65.38
21	Surplus	0.00
22	Reformulated Regular	677.44
23	Reformulated Premium	346.04
24	Conventional Regular	2985.70
25	Conventional Premium	1141.32
26	Surplus	0.00
27	Jet/Kero	1195.61
28	ULS Diesel	837.42
29	No.2 Oil	257.06
30	LSFO	431.15
31	LUBE stock	163.80
32	Jet/Kero copy	1340.30
33	NHT H2S	5.44
34	NHT Fuel Gas	12.67
35	LCNHT H2S	27.38
36	LCNHT Fuel Gas	85.21
37	H2 from Gasolene Reformer	1214.61
38	FG from Gasolene Reformer	59.59
39	NC3 from Gasolene Reformer	20.80
40	KHT H2S	6.81
41	KHT Fuel Gas	3.61
42	ARF Hydrogen	2265.44
43	ARF FG	139.05
44	ARF NC3	49.36
45	Benzene	38.52
46	Toluene	100.04
47	Xylenes	109.22
48	HDT H2S	19.73
49	DHT Fuel gas	19.92
50	GOHT H2S	294.15
51	GOHT Fuel Gas	47.43
52	DC H2S	8.38
53	DC FG	1290.65
54	Pet Coke	199.29
55	H2S from HCU	233.49
56	HCU Fuelgas	122.64
57	HCU C3s	19.25
58	FCC H2S	13.83

59	FCC Fuel Gas	668.19
60	FCC Coke	68.65
61	LCN to transfer	1323.47
62	H2S from C5 Isom	0.02
63	FG from C5 Isom	0.37
64	H2S from Scanfiner	0.41
65	Fuel Gas from Scanfiner	11.46
66	FG from C4 Isom	1.86
67	NC3 C4 Isom	0.58
	Total Physical Exergy OUT (kJ/s)	18923.941

Out of these 67 output streams, following are the streams with low amount of physical exergies, as shown in figure 4.3.

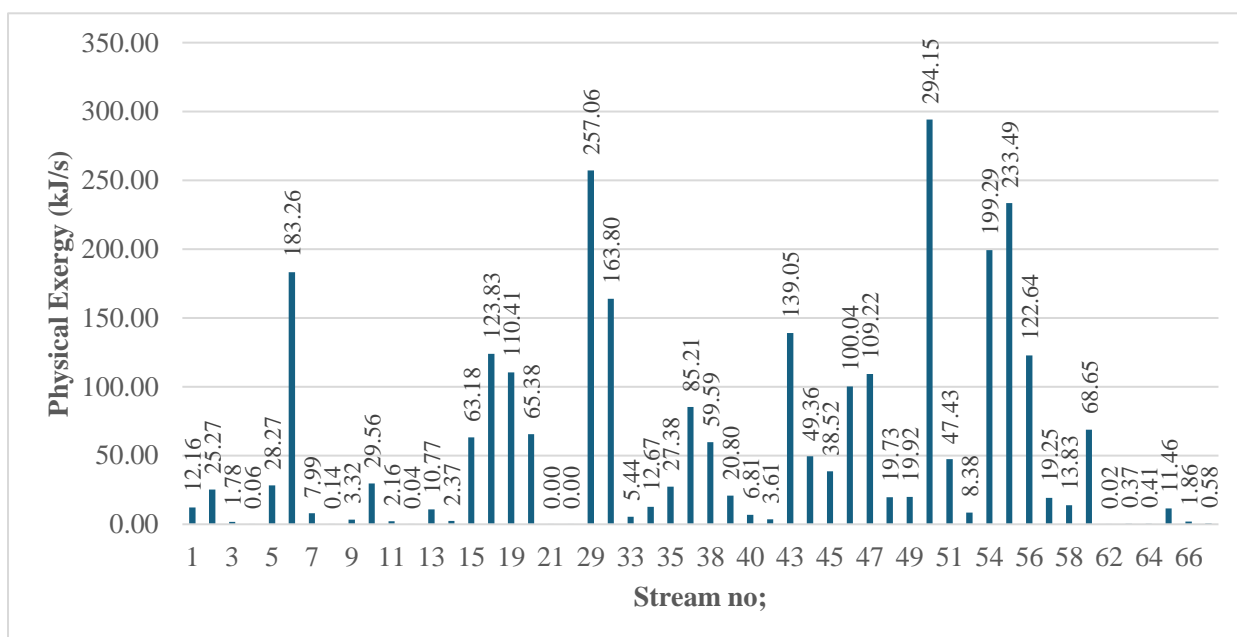


Figure 4.3: Output streams with low physical exergies

While the remaining streams which have the highest amount of exergy are shown graphically in the following figure 4.4.

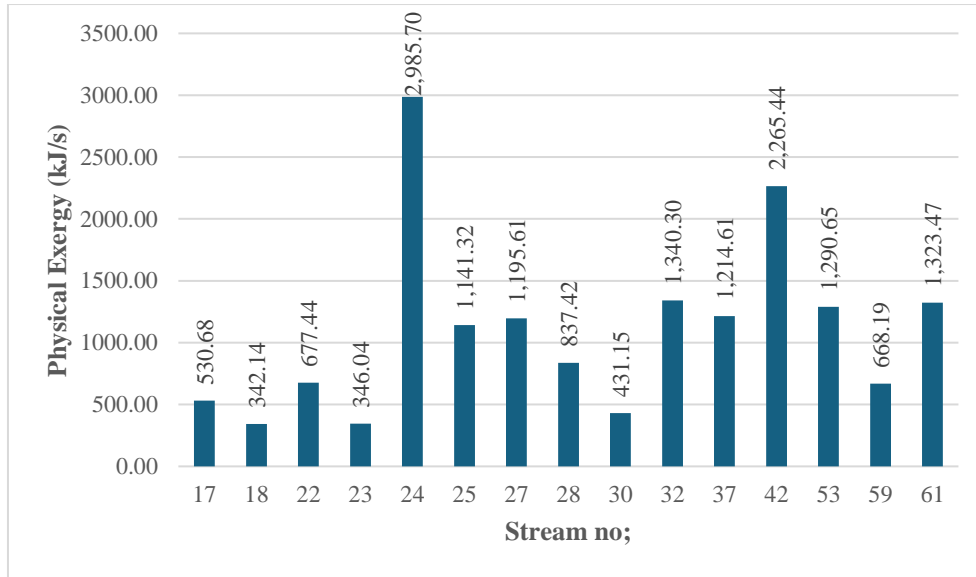


Figure 4.4: Output streams with high physical exergies

Hence the total Exergy IN and total Exergy OUT is calculated by the sum of exergies of all Input streams and all output streams respectively. Also, the overall plant wide Exergy destruction, Exergetic Improvement Potential, and Exergy efficiency were also calculated using equations no. (3.6), (3.7) and (3.8) respectively, as shown in Table below.

Total Phy Ex IN (kJ/s)	26235.92		
Total Phy Ex OUT (kJ/s)	18923.94		
Exergy Destruction (E_{xds}) (kJ/s)	E_x IN- E_x OUT		7311.98
Exergetic Improvement Potential (kJ/s)	$(1 - \eta) \times E_{xds}$		2037.85
Exergy Efficiency (η)	E_x OUT / E_x IN	0.721299014	72.13%

4.1.2 Exergetic improvement potential and irreversibility

The Exergy Destruction (E_{xds}), which represents the loss of useful energy due to inefficiencies in the system, is calculated as:

$$E_{xds} = E_x \text{ IN} - E_x \text{ OUT} = 26,235.92 \text{ kJ/s} - 18,923.94 \text{ kJ/s} = 7,311.98 \text{ kJ/s}$$

The Exergetic Improvement Potential, indicating the maximum possible improvement in the system's efficiency, is given by:

$$\text{Exergetic Improvement Potential} = (1 - \eta) \times \text{Ex}_{ds} = (1 - 0.7213) \times 7,311.98 \text{ kJ/s} = 2,037.85 \text{ kJ/s}$$

Figure 4.5 shows the exergetic improvement potential and exergy destruction or irreversibility of the petroleum refinery process. The exergetic improvement potential of the process is 7311.98 (kJ/s) and irreversibility of the process is 2037.85 (kJ/s).

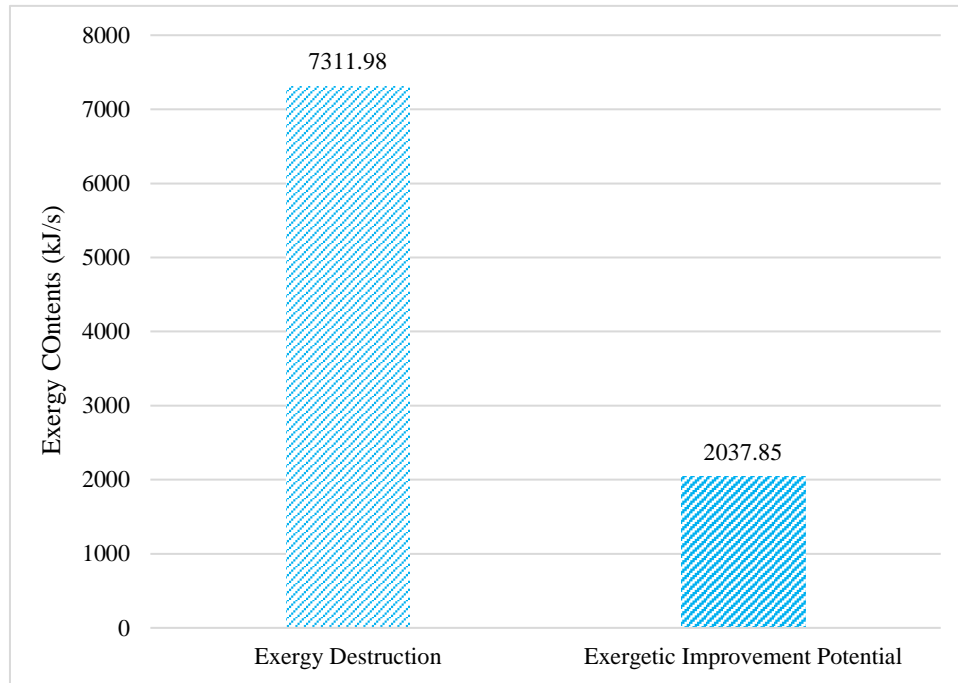


Figure 4.5: Exergetic improvement potential compared to irreversibility

4.1.3 Exergy efficiency

Exergy efficiency measures the system's efficacy relative to system performance. Figure 4.6 shows the exergy efficiency of the system. The Exergy Efficiency (η), which measures the fraction of input exergy that is effectively converted into useful output, is calculated as:

$$\eta = \text{Ex IN} / \text{Ex OUT}$$

$$\eta = 26,235.92 / 18,923.94 \text{ k} \approx 0.7213 \text{ or } 72.13\%$$

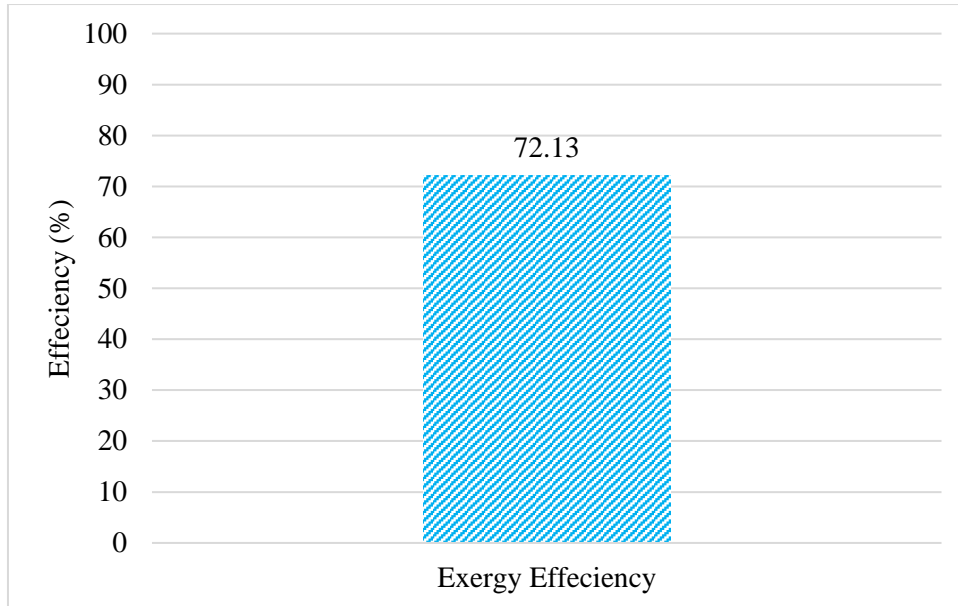


Figure 4.6: Steady state exergy efficiency of the system

4.2 Data based modelling and optimization

We conducted an examination of steady-state exergy in the preceding section. In this section, an artificial neural network was developed to predict the exergy efficiency and employed as a surrogate in evolutionary algorithm optimization framework to optimize the exergy efficiency under uncertainty.

4.2.1 ANN training validation and prediction of exergy efficiency

The ANN model was established in MATLAB R2021a. Uncertainty of -10% and +10% was inserted in 36 uncertain parameters. A total of 500 data sets were generated, out of which 400 were used for training, 50 for validation and 50 for model testing. ANN has trained with the scaled conjugate backpropagation (**trainsecg**) training algorithm while network behavior was controlled through the **Tansig** activation function. ANN model with one, two, and three hidden layers with varying numbers of neurons were iteratively tested to validate the best network architecture. The RMSE was used to quantify the performance of the model architecture. The model with three hidden layer and 60 50 40 neurons in 1st 2nd and 3rd hidden layers respectively were found to be the best design with the least RMSE, i.e, RMSE of 1.1349 for exergy efficiency.

The R value for training is 0.99925, for validation is 0.93288, and for testing 0.91209 as shown in the following Figure 4.7.

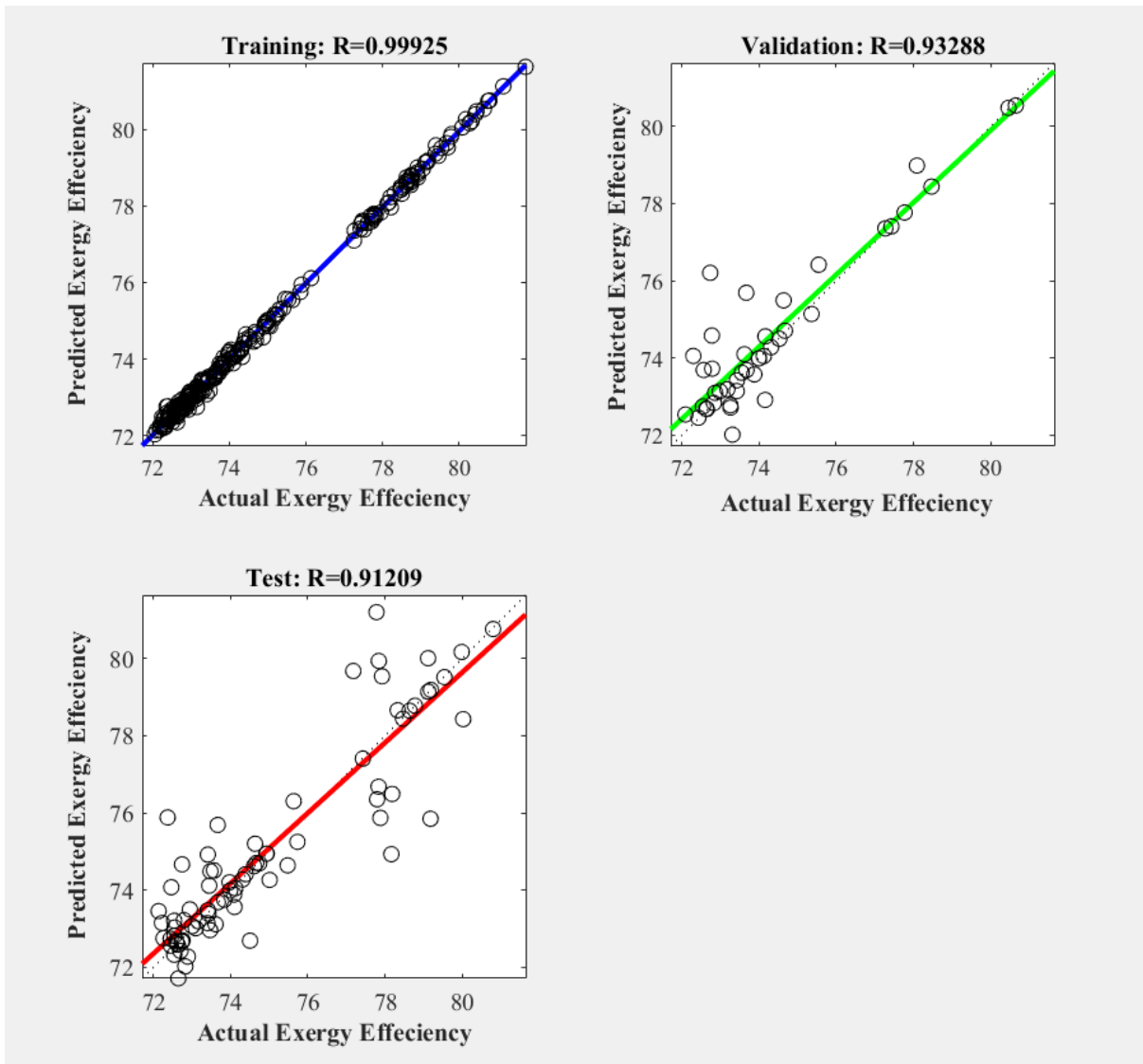


Figure 4.7: Predicted Vs actual exergy efficiency of training, testing and validation

The mean square error (MSE) were find out for validation performance, and it has the best validation performance value of 0.010847 at epoch no 860.

The value is shown in the following Figure 4.8 graphically.

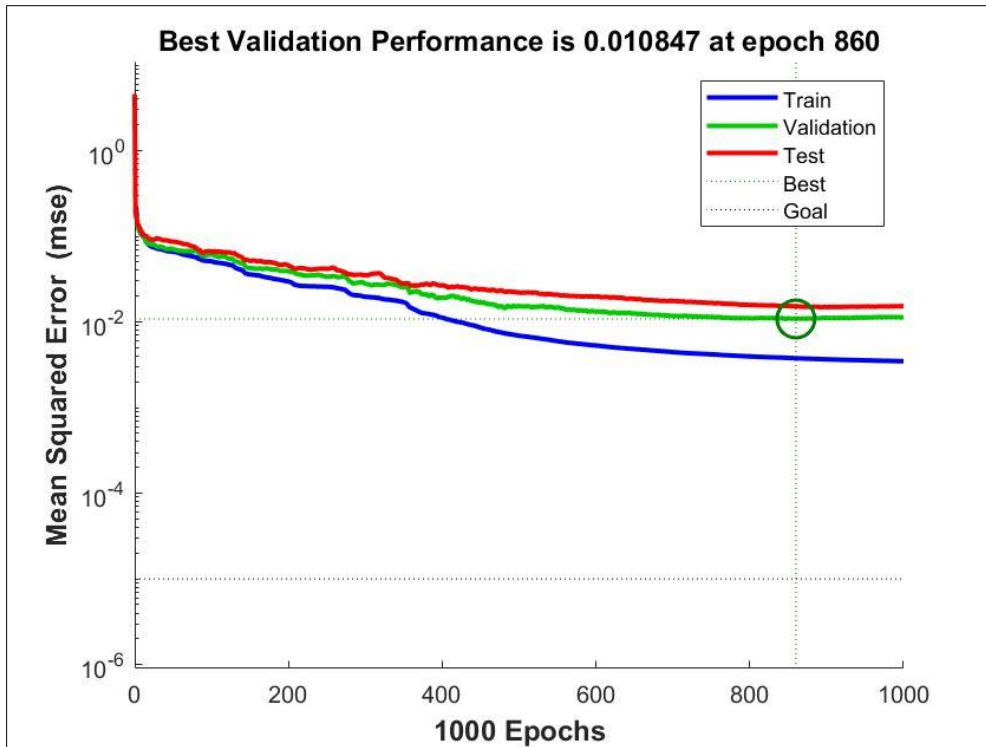


Figure 4.8: Validation performance

4.2.2 GA and PSO based optimization

Both the GA and PSO use ANN trained model as a surrogate to optimize the process exergy efficiency under uncertainty in process conditions. Table 4.3 and Table 4.4 present GA and PSO parameter used to optimize the process exergy efficiency.

GA parameters used to optimize the exergy efficiency for petroleum refining process are:

Initial Population: (150)

This is the number of candidate solutions (individuals) generated at the start of the algorithm. A larger initial population can provide a more diverse set of solutions, potentially leading to better overall optimization.

Crossover: (Over scatter)

Crossover, or recombination, is a genetic operator used to combine the genetic information of two parent solutions to generate new offspring. "Over scatter" likely refers to a method of spreading or distributing crossover points across the parent solutions to enhance diversity in the offspring.

Crossover Probability: (0.8)

This is the probability that two parent solutions will undergo crossover to produce offspring. A value of 0.8 means there is an 80% chance that crossover will occur, promoting exploration of new solutions.

Elite Member: (10)

This parameter specifies the number of top-performing individuals from each generation that are guaranteed to survive to the next generation. Elitism helps to ensure that the best solutions are preserved.

Mutation: (Adapt feasible)

Mutation introduces random changes to offspring solutions to maintain genetic diversity and explore new areas of the solution space. "Adapt feasible" suggests that mutations are adjusted or constrained to ensure that resulting solutions remain feasible and valid within the problem constraints.

Selection: (Tournament)

Tournament selection is a method where a subset of individuals from the population is randomly chosen, and the best individual from this subset is selected to contribute to the next generation. This method helps maintain selection pressure and diversity.

These parameters collectively guide the genetic algorithm in evolving solutions for optimizing the petroleum refining process, balancing exploration and exploitation to find the best possible outcomes.

Table 4.3: Genetic algorithm parameters used to optimize the exergy efficiency

GA parameters	Petroleum refining process
Initial population	150
Crossover	Over scatter
Crossover probability	0.8

Elite member	10
Mutation	Adapt feasible
Selection	Tournament

Following are the PSO parameters used to optimize the exergy efficiency for petroleum refining process:

Swarm Size: (200)

This is the number of particles in the swarm, each representing a potential solution to the optimization problem. A larger swarm size can increase the chances of finding an optimal solution by exploring a larger portion of the solution space.

Min Neighbours Fraction: (0.25)

This parameter defines the fraction of particles that each particle considers as its neighbors for social influence. A value of 0.25 means that each particle will interact with 25% of the swarm to update its position based on the performance of these neighbors, balancing local and global search.

Self Adjustment Weight: (1.49)

Also known as the cognitive or personal learning rate, this weight controls how much influence the particle's own best-known position (personal best) has on its movement. A value of 1.49 indicates the particle places a significant emphasis on its own previous experiences when adjusting its trajectory.

Social Adjustment Weight: (1.49)

Known as the social or global learning rate, this weight determines how much influence the best position found by any particle in the swarm (global best) has on a particle's movement. A

value of 1.49 suggests that particles are strongly influenced by the success of other particles in the swarm.

Initial Swarm Span: (2000)

This parameter sets the initial range within which the particles are randomly distributed in the solution space. A larger span of 2000 allows particles to explore a broader area of the search space initially, potentially improving the chances of finding a global optimum.

These parameters guide the behavior and performance of the PSO algorithm in optimizing the petroleum refining process, influencing how particles explore the solution space, learn from their own experiences and those of their neighbors, and adapt their positions to converge towards an optimal solution.

Table 4.4: PSO parameters used to optimize the exergy efficiency

PSO parameters	Petroelum refining process
Swarm size	200
Min; neighbours fraction	0.25
Self adjustment weight	1.49
Social adjustment weight	1.49
Initial swarm span	2000

4.2.3 Optimization of exergy efficiency

Table 4.5 shows a comparison of exergy efficiency of the process for GA and PSO based frameworks. Both the GA and PSO based frameworks outperformed in all test data samples in terms of exergy efficiency. For example, in data sample 1, it has an exergy efficiency of 77.43%, but the GA and PSO optimize it to 89.85% and 89.90%, respectively. Same case in data sample 2, where it has an exergy efficiency of 78.46%, but both the GA and PSO optimize it to 89.58% and 89.66%, respectively.

After that, the GA and PSO optimized data sets were fed up into Aspen HYSYS model for validation, and for the 1st data set sample, the value of Exergy efficiency is 88.23% upon GA solution data and 89.24% for PSO solution data. Same case for 2nd data set sample the exergy efficiency is 88.48% upon GA solution data and 89.48% for PSO solution data.

Then an absolute error were find out for GA and PSO predicted and validated cases. Like in data sample 1, the value of absolute error in case of GA is 0.02, while the value of absolute error in case of PSO is 0.01.

Table 4.5: Comparison of exergy efficiency of the process for GA and PSO

Data sets	Efficiency ($\pm 10\%$)	GA (Predicted)	PSO (Predicted)	ASPEN (Validation)	ASPEN (Validation)	Absolute difference for GA	Absolute difference for PSO
S.no				upon GA solution value	upon PSO solution value		
1	77.43	89.85	89.90	88.23	89.24	-0.02	-0.01
2	78.47	89.58	89.66	88.48	89.48	-0.01	0.00
3	79.12	88.72	89.17	88.18	88.39	-0.01	-0.01
4	72.63	84.94	85.11	82.93	83.58	-0.02	-0.02
5	72.64	84.69	84.74	82.83	83.06	-0.02	-0.02
6	72.70	85.19	85.27	83.08	84.09	-0.02	-0.01
7	72.71	84.87	84.93	81.05	81.05	-0.04	-0.05
8	73.99	85.28	85.59	82.09	83.27	-0.04	-0.03
9	79.19	87.79	87.88	86.52	86.56	-0.01	-0.01
10	72.74	85.03	85.96	84.07	84.37	-0.01	-0.02

The data set provides a comparison of predicted efficiency values obtained from Genetic Algorithms (GA) and Particle Swarm Optimization (PSO) against validation values from ASPEN simulations. It also includes the absolute differences between the predicted values and the ASPEN validation results

GA Predictions: The absolute differences between GA predictions and ASPEN validation values range from 0.01 to 0.04. This indicates that the GA predictions are generally very close to the ASPEN values.

PSO Predictions: The absolute differences between PSO predictions and ASPEN validation values range from 0.00 to 0.05. The PSO predictions are similarly close to the ASPEN values, with only slight variations.

For most data points, the differences between PSO predictions and ASPEN validation values are slightly smaller than those for GA predictions, indicating that PSO may have a marginal edge in accuracy for these particular cases. Both GA and PSO methods show consistent performance in approximating the ASPEN validation values. The differences are relatively small, suggesting both algorithms are effective in predicting efficiencies. Overall, the results suggest that both GA and PSO are effective in predicting efficiency values with high accuracy, and their predictions are consistently close to the ASPEN validation results.

The following figure 4.9 shows the comparison of exergy efficiencies of the process for GA predicted values and Aspen validated model upon GA solution values graphically.

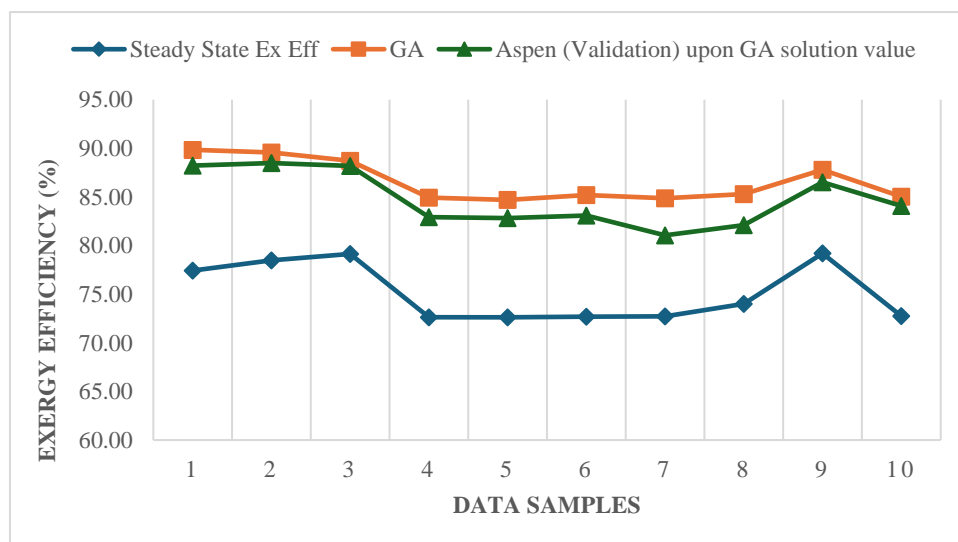


Figure 4.9: Comparison of exergy efficiency for steady state, GA, Aspen validated model

The following figure 4.10 graphically shows the comparison of exergy efficiencies of the process for PSO predicted values and Aspen validated model upon PSO solution values.

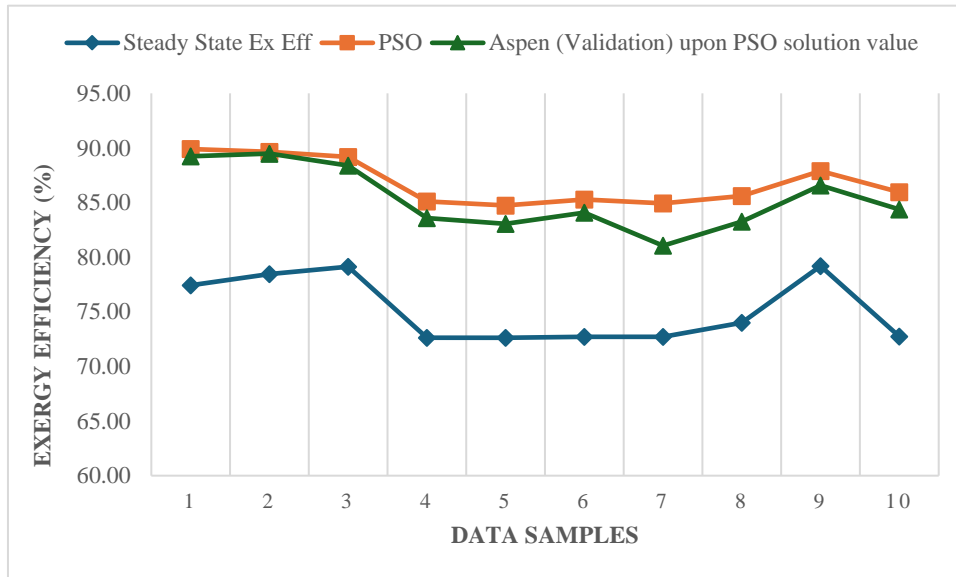


Figure 4.10: Comparison of exergy efficiency for steady state, PSO, Aspen validated model

In summary, both GA and PSO methods perform well in predicting efficiencies with minimal absolute differences from ASPEN validation values. The PSO method shows slightly better accuracy in this dataset, but the differences are generally very small for both methods.

CHAPTER 05: CONCLUSIONS

The steady state exergy efficiency of overall petroleum refinery plant model is 72.13%, while the exergy destruction or irreversibility of the plant wide model is 7311.97 kW and the exergetic improvement potential is 2037.85 kW. After finding out the steady state exergy analysis, an ANN code was established in MATLAB, under uncertainty of $\pm 10\%$ in 36 hyperparameters. 500 data samples were generated, in which 400 were used for training, and 50 50 were used for testing and validation of the model. Then an ANN model was developed and used as a surrogate in a GA and PSO environment for optimization under uncertainty where exergy efficiency was the objective function. The RMSE was used to quantify the performance of the model architecture, having RMSE of 1.1349 for exergy efficiency. The R value for Training is 0.99925, for Validation is 0.93288, and for testing 0.91209. The framework overtook steady state model in achieving the highest exergy efficiency. The performance of both algorithms was cross-validated by putting the optimized solution value on the Aspen HYSYS model and getting the absolute error. Overall, the performance of the PSO and GA were comparable, and it was concluded that the PSO performed marginally better than the GA. The suggested surrogate-based optimization technique will serve as a framework for implementing industry 4.0 in the petroleum refinery at the plant level.

REFERENCES

- [1] F. Bühler, T. Van Nguyen, and B. Elmegaard, “Energy and exergy analyses of the Danish industry sector,” *Appl Energy*, vol. 184, pp. 1447–1459, Dec. 2016, doi: 10.1016/j.apenergy.2016.02.072.
- [2] E. S. Dogbe, M. A. Mandegari, and J. F. Görgens, “Exergetic diagnosis and performance analysis of a typical sugar mill based on Aspen Plus® simulation of the process,” *Energy*, vol. 145, pp. 614–625, Feb. 2018, doi: 10.1016/j.energy.2017.12.134.
- [3] M. Aghbashlo, H. Mobli, S. Rafiee, and A. Madadlou, “A review on exergy analysis of drying processes and systems,” *Renewable and Sustainable Energy Reviews*, vol. 22, pp. 1–22, 2013. doi: 10.1016/j.rser.2013.01.015.
- [4] G. Boroumandjazi, B. Rismanchi, and R. Saidur, “A review on exergy analysis of industrial sector,” *Renewable and Sustainable Energy Reviews*, vol. 27. Elsevier Ltd, pp. 198–203, 2013. doi: 10.1016/j.rser.2013.06.054.
- [5] P. Luis and B. Van der Bruggen, “Exergy analysis of energy-intensive production processes: Advancing towards a sustainable chemical industry,” *Journal of Chemical Technology and Biotechnology*, vol. 89, no. 9. John Wiley and Sons Ltd, pp. 1288–1303, 2014. doi: 10.1002/jctb.4422.
- [6] T. Taner and M. Sivrioglu, “Energy-exergy analysis and optimisation of a model sugar factory in Turkey,” *Energy*, vol. 93, pp. 641–654, Dec. 2015, doi: 10.1016/j.energy.2015.09.007.
- [7] N. A. Madloul, R. Saidur, N. A. Rahim, and M. Kamalisarvestani, “An overview of energy savings measures for cement industries,” *Renewable and Sustainable Energy Reviews*, vol. 19, pp. 18–29, 2013. doi: 10.1016/j.rser.2012.10.046.
- [8] M. Macedo Costa, R. Schaeffer, and E. Worrell, “Exergy accounting of energy and materials flows in steel production systems,” 2001. [Online]. Available: www.elsevier.com/locate/energy
- [9] V. A. F. Costa, L. A. C. Tarelho, and A. Sobrinho, “Mass, energy and exergy analysis of a biomass boiler: A portuguese representative case of the pulp and paper industry,” *Appl*

- Therm Eng*, vol. 152, pp. 350–361, Apr. 2019, doi: 10.1016/j.applthermaleng.2019.01.033.
- [10] J. F. Portha, S. Louret, M. N. Pons, and J. N. Jaubert, “Estimation of the environmental impact of a petrochemical process using coupled LCA and exergy analysis,” *Resour Conserv Recycl*, vol. 54, no. 5, pp. 291–298, Mar. 2010, doi: 10.1016/j.resconrec.2009.09.009.
- [11] J. Mustafa, I. Ahmad, M. Ahsan, and M. Kano, “Computational fluid dynamics based model development and exergy analysis of naphtha reforming reactors,” *International Journal of Exergy*, vol. 24, no. 2–4, pp. 344–363, 2017, doi: 10.1504/IJEX.2017.087696.
- [12] M. Nuhu, A. S. Olawale, N. Salahudeen, A. Z. Yusuf, and Y. Mustapha, “Exergy and Energy Analysis of Fluid Catalytic Cracking Unit in Kaduna Refining and Petrochemical Company,” *International Journal of Chemical Engineering and Applications*, pp. 441–445, 2012, doi: 10.7763/IJCEA.2012.V3.239.
- [13] Petar Sabev Varbanov and Jiri Klemeš, “Exergy Analysis Applied to Separation Processes in a FCC Plant Using Computational Models”.
- [14] Q. L. Chen, Q. H. Yin, S. P. Wang, and B. Hua, “Energy-use analysis and improvement for delayed coking units,” in *Energy*, Elsevier Ltd, 2004, pp. 2225–2237. doi: 10.1016/j.energy.2004.03.021.
- [15] Y. Lei, D. Zeng, and G. Wang, “Improvement potential analysis for integrated fractionating and heat exchange processes in delayed coking units,” *Chin J Chem Eng*, vol. 24, no. 8, pp. 1047–1055, Aug. 2016, doi: 10.1016/j.cjche.2016.04.038.
- [16] M. Khan, I. Ahmad, M. Ahsan, M. Kano, and H. Caliskan, “Prediction of optimum operating conditions of a furnace under uncertainty: An integrated framework of artificial neural network and genetic algorithm,” *Fuel*, vol. 330, Dec. 2022, doi: 10.1016/j.fuel.2022.125563.
- [17] T. Gueddar and V. Dua, “Novel model reduction techniques for refinery-wide energy optimisation,” *Appl Energy*, vol. 89, no. 1, pp. 117–126, 2012, doi: 10.1016/j.apenergy.2011.05.056.

- [18] A. U. Akram, I. Ahmad, A. Chughtai, and M. Kano, “Exergy analysis and optimisation of naphtha reforming process with uncertainty,” *International Journal of Exergy*, vol. 26, no. 3, pp. 247–262, 2018, doi: 10.1504/IJEX.2018.093138.
- [19] A. Samad, I. Ahmad, M. Kano, and H. Caliskan, “Prediction and optimization of exergetic efficiency of reactive units of a petroleum refinery under uncertainty through artificial neural network-based surrogate modeling,” *Process Safety and Environmental Protection*, vol. 177, pp. 1403–1414, Sep. 2023, doi: 10.1016/j.psep.2023.07.046.
- [20] A. Samad and I. Ahmad, “An Intelligent System for Estimation of Exergy Efficiency of Integrated Naphtha and Isomerization Process under Uncertainty,” in *2022 17th International Conference on Emerging Technologies, ICET 2022*, Institute of Electrical and Electronics Engineers Inc., 2022, pp. 12–17. doi: 10.1109/ICET56601.2022.10004625.
- [21] A. Hepbasli, “A key review on exergetic analysis and assessment of renewable energy resources for a sustainable future,” *Renewable and Sustainable Energy Reviews*, vol. 12, no. 3, pp. 593–661, Apr. 2008. doi: 10.1016/j.rser.2006.10.001.
- [22] Y. M. , & D. I. (2013). El-Sayed, “Exergy analysis of petroleum refining and evaluation of its sustainability performance. *Energy Conversion and Management*”.
- [23] A. H. Tambunan and A. Subiyanto, “Exergy Analysis for Sustainable Improvement of Crude Oil Distillation Process in Refinery. *Energy Procedia*,” pp. 5221-5226., 2020.
- [24] J. Szargut, D. R. Morris, and F. R. Steward, “Exergy Analysis of Thermal, Chemical, and Metallurgical Processes. Hemisphere Publishing Corporation.,” 1988.
- [25] Z. Jia and M. G. Ierapetritou, “Modeling and Optimization of Refinery Operations Considering Uncertainty,” in *Process Systems Engineering*, Wiley, 2007, pp. 219–235. doi: 10.1002/9783527631278.ch7.
- [26] A. Al-Shammari and M. S. Ba-Shammakh, “Uncertainty analysis for refinery production planning,” *Ind Eng Chem Res*, vol. 50, no. 11, pp. 7065–7072, Jun. 2011, doi: 10.1021/ie200313r.

- [27] L. De Pádua Agripa Sales, F. M. T. De Luna, and B. De Athayde Prata, “An integrated optimization and simulation model for refinery planning including external loads and product evaluation,” *Brazilian Journal of Chemical Engineering*, vol. 35, no. 1, pp. 199–215, Jan. 2018, doi: 10.1590/0104-6632.20180351s20160124.
- [28] D. Iranshahi, M. Karimi, S. Amiri, M. Jafari, R. Rafiei, and M.R.J.C.E.R. Rahimpour, “Design, Modeling of naphtha reforming unit applying detailed description of kinetic in continuous catalytic regeneration process,” pp. 1704–1727, 2014.
- [29] M. R. Rahimpour, M. Jafari, and D. Iranshahi, “Progress in catalytic naphtha reforming process: A review,” *Applied Energy*, vol. 109. Elsevier Ltd, pp. 79–93, 2013. doi: 10.1016/j.apenergy.2013.03.080.
- [30] J. H. Gary, J. H. Handwerk, M. J. Kaiser, and D. Geddes, *Petroleum Refining*. CRC Press, 2007. doi: 10.4324/9780203907924.
- [31] L. C. Castañeda, J. A. D. Muñoz, and J. Ancheyta, “Combined process schemes for upgrading of heavy petroleum,” *Fuel*, vol. 100, pp. 110–127, Oct. 2012, doi: 10.1016/j.fuel.2012.02.022.
- [32] C. Ferreira *et al.*, “Modeling residue hydrotreating,” *Chem Eng Sci*, vol. 65, no. 1, pp. 322–329, Jan. 2010, doi: 10.1016/j.ces.2009.06.062.
- [33] P.R. Robinson, *Practical Advances in Petroleum Processing*. New York, NY: Springer New York, 2006. doi: 10.1007/978-0-387-25789-1.
- [34] S. R. Naqvi *et al.*, “New trends in improving gasoline quality and octane through naphtha isomerization: a short review,” *Appl Petrochem Res*, vol. 8, no. 3, pp. 131–139, Sep. 2018, doi: 10.1007/s13203-018-0204-y.
- [35] V. A. Chuzlov, E. D. Ivanchina, I. M. Dolganov, and K. V. Molotov, “Simulation of Light Naphtha Isomerization Process,” *Procedia Chem*, vol. 15, pp. 282–287, 2015, doi: 10.1016/j.proche.2015.10.045.
- [36] J.G. Speight, “The refinery of the future,” in *The Refinery of the Future*, Elsevier, 2011, pp. 389–395. doi: 10.1016/B978-0-8155-2041-2.10012-8.

- [37] M. Golmohammadi, S. J. Ahmadi, and J. Towfighi, "Catalytic cracking of heavy petroleum residue in supercritical water: Study on the effect of different metal oxide nanoparticles," *J Supercrit Fluids*, vol. 113, pp. 136–143, Jul. 2016, doi: 10.1016/j.supflu.2016.03.023.
- [38] B. Sankararao and S. K. Gupta, "Multi-objective optimization of an industrial fluidized-bed catalytic cracking unit (FCCU) using two jumping gene adaptations of simulated annealing," *Comput Chem Eng*, vol. 31, no. 11, pp. 1496–1515, Nov. 2007, doi: 10.1016/j.compchemeng.2006.12.012.
- [39] R. Gupta, V. Kumar, and V. K. Srivastava, "MODELING AND SIMULATION OF FLUID CATALYTIC CRACKING UNIT," *Reviews in Chemical Engineering*, vol. 21, no. 2, Jan. 2005, doi: 10.1515/REVCE.2005.21.2.95.
- [40] M. A. Ali, T. Tatsumi, and T. Masuda, "Development of heavy oil hydrocracking catalysts using amorphous silica-alumina and zeolites as catalyst supports," *Appl Catal A Gen*, vol. 233, no. 1–2, pp. 77–90, Jul. 2002, doi: 10.1016/S0926-860X(02)00121-7.
- [41] S. Mohanty, D. Kunzru, and D. N. Saraf, "Hydrocracking: a review," *Fuel*, vol. 69, no. 12, pp. 1467–1473, 1990, doi: [https://doi.org/10.1016/0016-2361\(90\)90192-S](https://doi.org/10.1016/0016-2361(90)90192-S).
- [42] K. H. Kang *et al.*, "Slurry-phase hydrocracking of heavy oil over Mo precursors: Effect of triphenylphosphine ligands," *J Catal*, vol. 384, pp. 106–121, Apr. 2020, doi: 10.1016/j.jcat.2020.02.007.
- [43] M. S. Rana, V. Sámano, J. Ancheyta, and J. A. I. Diaz, "A review of recent advances on process technologies for upgrading of heavy oils and residua," *Fuel*, vol. 86, no. 9, pp. 1216–1231, Jun. 2007, doi: 10.1016/j.fuel.2006.08.004.
- [44] E. Furimsky, "Characterization of cokes from fluid/flexi-coking of heavy feeds," *Fuel Processing Technology*, vol. 67, no. 3, pp. 205–230, Sep. 2000, doi: 10.1016/S0378-3820(00)00103-X.
- [45] V. R. Botelho *et al.*, "Model assessment of MPCs with control ranges: An industrial application in a delayed coking unit," *Control Eng Pract*, vol. 84, pp. 261–273, Mar. 2019, doi: 10.1016/j.conengprac.2018.11.003.

- [46] Q. CHEN, “Energy-use analysis and improvement for delayed coking units,” *Energy*, vol. 29, no. 12–15, pp. 2225–2237, Dec. 2004, doi: 10.1016/j.energy.2004.03.021.
- [47] P. J. Ellis and C. A. Paul, “Tutorial: Delayed Coking Fundamentals,” 1998. [Online]. Available: <https://api.semanticscholar.org/CorpusID:137875679>
- [48] S. Enrico, E. Sciubba, and G. Wall, “A brief Commented History of Exergy From the Beginnings to 2004,” *Article in International Journal of Thermodynamics*, vol. 10, no. 1, pp. 1–26, 2007, doi: 10.5541/ijot.184.
- [49] A. Naeimi, M. Bidi, M. H. Ahmadi, R. Kumar, M. Sadeghzadeh, and M. Alhuyi Nazari, “Design and exergy analysis of waste heat recovery system and gas engine for power generation in Tehran cement factory,” *Thermal Science and Engineering Progress*, vol. 9, pp. 299–307, Mar. 2019, doi: 10.1016/j.tsep.2018.12.007.
- [50] C. Yan, L. Lv, S. Wei, A. Eslamimanesh, and W. Shen, “Application of retrofitted design and optimization framework based on the exergy analysis to a crude oil distillation plant,” *Appl Therm Eng*, vol. 154, pp. 637–649, May 2019, doi: 10.1016/j.applthermaleng.2019.03.128.
- [51] E. S. Dogbe, M. A. Mandegari, and J. F. Görgens, “Exergetic diagnosis and performance analysis of a typical sugar mill based on Aspen Plus® simulation of the process,” *Energy*, vol. 145, pp. 614–625, Feb. 2018, doi: 10.1016/j.energy.2017.12.134.
- [52] A. Al-Shathr, Z. M. Shakor, H. S. Majdi, A. A. Abdulrazak, and T. M. Albayati, “Comparison between artificial neural network and rigorous mathematical model in simulation of industrial heavy naphtha reforming process,” *Catalysts*, vol. 11, no. 9, Sep. 2021, doi: 10.3390/catal11091034.
- [53] H. P. Gavin, “The Levenberg-Marquardt algorithm for nonlinear least squares curve-fitting problems,” 2022.
- [54] S. Katoch, S. S. Chauhan, and V. Kumar, “A review on genetic algorithm: past, present, and future,” *Multimed Tools Appl*, vol. 80, no. 5, pp. 8091–8126, Feb. 2021, doi: 10.1007/s11042-020-10139-6.

- [55] M. Kumar, M. Husian, N. Upreti, and D. Gupta, "GENETIC ALGORITHM: REVIEW AND APPLICATION." [Online]. Available: <https://ssrn.com/abstract=3529843>
- [56] K. Jebari and M. Madiafi, "Selection Methods for Genetic Algorithms," *Int. J. Emerg. Sci*, vol. 3, no. 4, pp. 333–344, 2013, [Online]. Available: <https://www.researchgate.net/publication/259461147>
- [57] S. Sadighi, R. S. Mohaddecy, and A. Norouzian, "Optimizing an industrial scale naphtha catalytic reforming plant using a hybrid artificial neural network and genetic algorithm technique," *Bulletin of Chemical Reaction Engineering and Catalysis*, vol. 10, no. 2, pp. 210–220, 2015, doi: 10.9767/bcrec.10.2.7171.210-220.